

**Biospectroscopy reveals the effect of varying water quality on tadpole tissues of the Common Frog (*Rana temporaria*)**

Rebecca Strong<sup>1</sup>, Crispin J. Halsall<sup>1\*</sup>, Martin Ferenčík<sup>2,3</sup>, Kevin C. Jones<sup>1</sup>, Richard F. Shore<sup>4</sup> and Francis L. Martin<sup>1\*</sup>

<sup>1</sup>*Lancaster Environment Centre, Lancaster University, Bailrigg, Lancaster LA1 4YQ, UK*

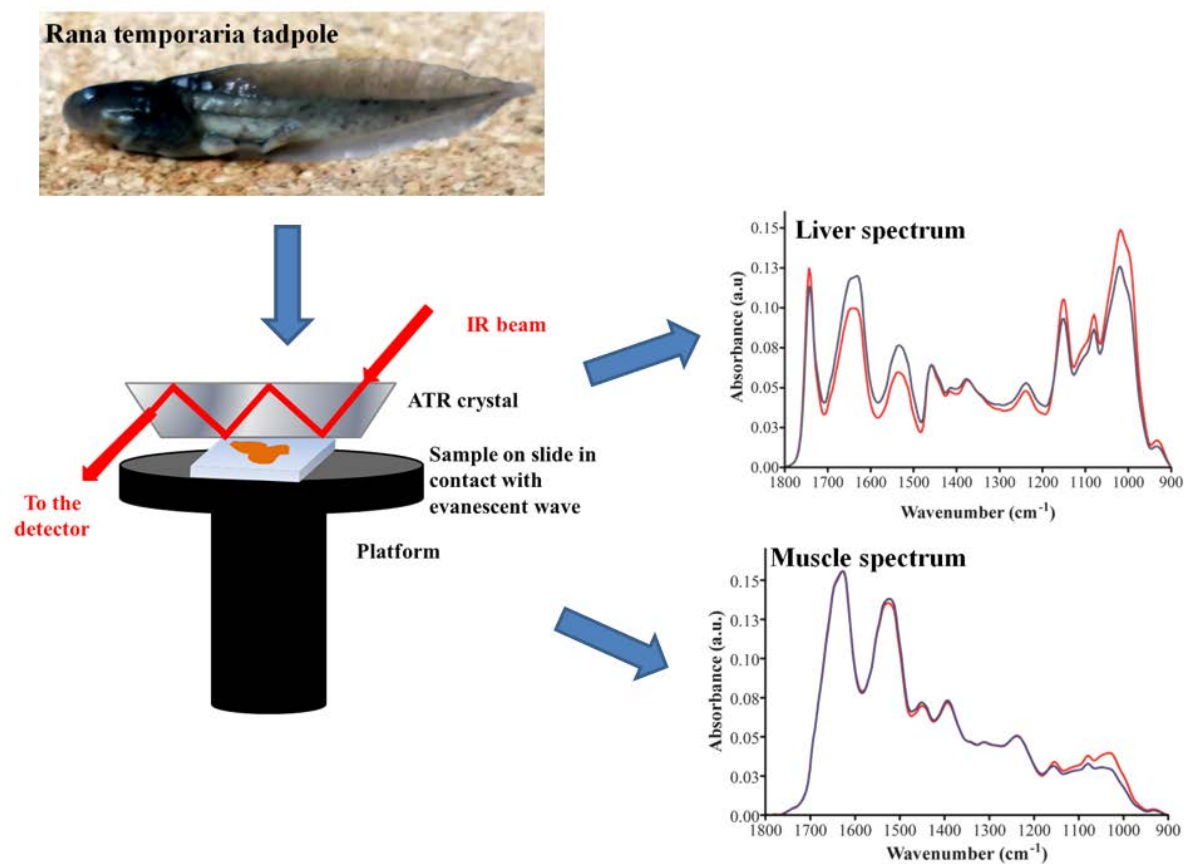
<sup>2</sup>*Povodí Labe, státní podnik, Odbor vodohospodářských laboratorý (OVHL), Víta Nejedlého 951, 500 03 Hradec Králové, Czech Republic*

<sup>3</sup>*Institute of Environmental and Chemical Engineering, Faculty of Chemical Technology, University of Pardubice, Studentská 573, 532 10 Pardubice, Czech Republic*

<sup>4</sup>*Centre for Ecology and Hydrology, Lancaster University, Bailrigg, Lancaster LA1 4YQ, UK*

\* Corresponding authors. Email address: [c.halsall@lancaster.ac.uk](mailto:c.halsall@lancaster.ac.uk) (C.J. Halsall);  
[f.martin@lancaster.ac.uk](mailto:f.martin@lancaster.ac.uk) (F.L. Martin).

## Graphical abstract



## Highlights

- Comparison of ponds with differing water quality in the UK
- ATR-FTIR spectroscopy detects spectral alterations in common frog tadpoles
- Spectral alterations detected in several tissues; liver is most sensitive
- Liver size also potentially affected by agricultural pollutant exposure

## Abstract

Amphibians are undergoing large population declines in many regions around the world. As environmental pollution from both agricultural and urban sources has been implicated in such declines, there is a need for a biomonitoring approach to study potential impacts on this vulnerable class of organism. This study assessed the use of infrared (IR) spectroscopy as a tool to detect changes in several tissues (liver, muscle, kidney, heart and skin) of late-stage common frog (*Rana temporaria*) tadpoles collected from ponds with differing water quality. Small differences in spectral signatures were revealed between a rural agricultural pond and an urban pond receiving wastewater and landfill run-off; these were limited to the liver and heart, although large differences in body size were apparent, surprisingly with tadpoles from the urban site larger than those from the rural site. Large differences in liver spectra were found between tadpoles from the pesticide and nutrient impacted pond compared to the rural agricultural pond, particularly in regions associated with lipids. Liver mass and hepatosomatic indices were found to be significantly increased in tadpoles from the site impacted by pesticides and trace organic chemicals, suggestive of exposure to environmental contamination. Significant alterations were also found in muscle tissue between tadpoles from these two ponds in regions associated with glycogen, potentially indicative of a stress response. This study highlights the use of IR spectroscopy, a low-cost, rapid and reagent-free technique in the biomonitoring of a class of organisms susceptible to environmental degradation.

**Keywords:** Amphibian declines; Environmental pollution; IR spectroscopy; Liver; Tadpoles

**Capsule:** Infrared spectroscopy was used as a tool to detect contaminant-induced alterations in pro-metamorphic tadpoles of the common frog in a range of tissues.

## Introduction

Amphibians are facing large declines globally, with a number of hypotheses proposed to explain such declines, including habitat destruction, disease, climate change, UV radiation, predation and environmental contamination (Beebee and Griffiths, 2005; Blaustein et al., 2003; Mann et al., 2009; Stuart et al., 2004). Whilst no one factor is likely to be the sole cause of population decreases (Blaustein et al., 2011), it is known that amphibians may be particularly vulnerable to environmental contamination as their reproduction and larval development occurs in aquatic habitats, often adjacent to surface run-off from agricultural and urban sources (Mann et al., 2009; Ralph and Petras, 1997). This coupled with the permeable skin of amphibians, offering little protection against toxic contaminants (Blaustein et al., 2003), means that they are regarded as indicators of environmental stress (Blaustein and Wake, 1995).

While amphibians are considered to be most vulnerable to environmental stress during early tadpole development (Bridges, 2000; Greulich and Pflugmacher, 2003), the effects of such exposure may have consequences in later development (Bridges, 2000; Orton and Routledge, 2011; Orton and Tyler, 2014). This could include a smaller size at metamorphosis, exposing the juvenile amphibian to an increased risk of predation, or delayed development and metamorphosis, which could mean that the ephemeral ponds dry up before metamorphosis occurs (Altwegg and Reyer, 2003; Egea-Serrano et al., 2012; Hayes et al., 2006; Venturino et al., 2003). Thus, it is useful to determine the effects in the later stages of development prior to metamorphic climax.

A technique increasingly being employed to derive detailed information from biological samples is Fourier-transform infrared (FTIR) spectroscopy, which is used in three major sampling modes: transmission, reflectance and attenuated total reflectance (ATR) (Kazarian

and Chan, 2006). FTIR spectroscopy has been widely used in several biological applications including the diagnosis of disease states (Baker et al., 2014; Bellisola and Sorio, 2012; Ellis and Goodacre, 2006; Kazarian and Chan, 2006; Movasaghi et al., 2008; Toyran et al., 2006), imaging of tissue composition (Greve et al., 2008; Purna Sai and Babu, 2001), identifying microorganisms (Mariey et al., 2001; Naumann et al., 1991) and for analysing the effects of environmental contaminants at the cellular and tissue level (Abdel-Gawad et al., 2012; Cakmak et al., 2006; Cakmak et al., 2003; Corte et al., 2010; Holman et al., 2000; Llabjani et al., 2012; Malins et al., 2006; Obinaju et al., 2014; Palaniappan and Vijayasundaram, 2008, 2009; Palaniappan et al., 2011; Ukpebor et al., 2011).

The basic principle of FTIR spectroscopy is that when a sample is analysed with an IR beam, the functional groups within the sample vibrate in different ways in the mid-IR region: stretching (asymmetric or symmetric) or deformations (mainly asymmetric and symmetric bending) (Bellisola and Sorio, 2012). The absorption can then be correlated to particular biochemical entities (*e.g.*, DNA/RNA, carbohydrate, proteins and lipids) and the resultant spectrum viewed as an infrared fingerprint (Ellis and Goodacre, 2006). Using IR spectroscopy is advantageous as this technique is label-free, thus allowing samples to be used subsequently for other applications, rapid, reagent-free, and cost-effective as minimal sample preparation is required (Baker et al., 2014; Kazarian and Chan, 2006).

FTIR spectroscopy generates large detailed datasets so is often coupled with a multivariate approach such as principal component analysis (PCA) or linear discriminant analysis (LDA) to extract useful information from the resulting IR absorbance spectrum (Ellis and Goodacre, 2006). Used in this manner, FTIR spectroscopy is able to distinguish between different groups on the basis of their biochemical fingerprint and also identifies which wavenumbers, and therefore which chemical bonds are altered between samples (Trevisan et al., 2012). Additionally, use of derivative spectra may allow more detailed examination of overlapping

peaks in the spectrum, thus allowing the quantification of particular biochemical constituents (Rieppo et al., 2012).

The aim of this study was to determine whether tadpoles of the Common frog, *Rana temporaria*, at a pro-metamorphic stage in development. i.e. following the emergence and development of hindlimbs [Gosner stage 38-40 (Gosner, 1960)] collected from ponds with varying water quality could be distinguished on the basis of their ATR-FTIR spectral fingerprint. Detection of underlying differences may suggest the possible application of IR spectroscopy as an environmental monitoring tool. Liver and muscle samples were taken from individual tadpoles and analysed with ATR-FTIR spectroscopy; previous studies in amphibians using other techniques have demonstrated changes in metabolic constituents such as lipid, protein and glycogen following exposure to environmental contaminants in these tissues (Dornelles and Oliveira, 2014; Gendron et al., 1997; Gurushankara et al., 2007; Melvin et al., 2013). Other tissues less routinely used in assessing amphibian health (heart, kidney and skin) were also analysed in this study, thus providing spectral fingerprints of several different tissues of an amphibian species. Although applied to fish in several studies (Cakmak et al., 2006; Henczova et al., 2008; Malins et al., 2006; Malins et al., 2004; Obinaju et al., 2014), this is the first time to our knowledge that IR spectroscopy has been used to characterise amphibian tissue.

## **Materials and Methods**

### **Pond Selection**

Sites were selected in order to give a comparison between agricultural and urban ponds and were based on site characteristics and information from landowners/land managers.

1. Whinton Hill (WH), Plumpton, Cumbria is a farm consisting primarily of arable land, which is routinely sprayed with herbicides and fungicides. The pond surveyed was the shallow pond of a pair of deep and shallow ponds (32 m long  $\times$  8 m wide  $\times$  0.5 m deep), located in a boggy field, and fed by a field drain from approximately 30 ha ( $3 \times 10^5 \text{ m}^2$ ) of farmland.

2. Crake Trees (CT), Crosby Ravensworth is a farm used as beef grazing land and marginal arable land, which has been accepted onto Natural England's Higher Level Environmental Stewardship Scheme and uses minimal quantities of pesticides, with buffer zones to prevent pesticide run-off into water courses. The pond surveyed was the second pond of a pair of shallow ponds (each 17 m long  $\times$  6 m wide  $\times$  0.5 m deep), located in a field corner, and fed by surface runoff from approximately 20 ha ( $2 \times 10^5 \text{ m}^2$ ) of farmland.

The ponds surveyed at WH and CT are part of the MOPS2 (Mitigation Options for Phosphorus and Sediment) project monitored by Lancaster University (<http://mops2.diffusepollution.info/>).

3. Pennington Flash Country Park (PF) located in Leigh, Lancashire is a site managed by Wigan and Leigh Culture Trust. The 'Flash' is a large lake formed over time by mining subsidence. The southern part of the Flash was filled with domestic waste during the 1950s to prevent the regular flooding of nearby St Helen's Road. The pond sampled is adjacent to Westleigh Brook, which receives treated wastewater from Leigh wastewater treatment works.

## **Water sampling**

Samples of surface water (15-20 cm depth) were collected over the amphibian breeding season (March-August) in 2012. Water samples for organics analysis were only available from PF for March and April, and March, April and June for nutrient analysis. Water samples

were collected in methanol-rinsed amber bottles for organics analysis and acid-washed bottles for nutrient analysis and then stored at 4°C until analysis.

## **Chemical analysis**

The concentrations of trace metals (Al, Fe, Mg, Ca, K and Na) were determined in filtered acidified water samples (1% HNO<sub>3</sub>) using ICP-OES (Perkin Elmer DV 7300) while concentrations of major anions (Cl, NO<sub>3</sub>-N, SO<sub>4</sub>-S) as well as phosphate, ammonium and total organic N (TON) were determined using colorimetric methods performed by the Centre for Ecology and Hydrology (Lancaster) in a quality-assured, previously published method (Neal et al., 2000). For trace organic chemical analysis, 800 mL of sample water (adjusted to pH 9.5 with borate buffer) underwent liquid-liquid (1:1) extraction using dichloromethane (DCM) on a laboratory shaker (Gerhardt Shaker LS-500) followed by separation and evaporation of the DCM on a rotary evaporator (rotavapor Büchi R-210). The concentrated DCM extracts (700 µL) underwent initial qualitative screening using GC-MS (Agilent 6890N GC and Agilent 5973 single quad MS) operated by ChemStation software (D.02.00.275) with subsequent mass spectral identification using Mass Hunter software and comparison to the NIST spectral library. The following chemicals were detected: aniline, metazachlor, acetochlor, dimetachlor, triethylphosphate, tributylphosphate, tris(2-chloroethyl)phosphate, tris(1-chloro-2-propyl)phosphate and flusilazole. These compounds were quantitatively analysed using authentic standards using a 7-point calibration, with standards ranging from 0-2000 ng/L for each analyte. Internal standards comprising of <sup>13</sup>C-labelled aniline, acetochlor and metalochlor were added to sample extracts and calibration standards prior to analysis. Limits of quantification (LOQ) ranged from 5-10 ng/L (aniline 200 ng/L) with recoveries based on spiked water samples ranging from 80-120%. Water samples were also analysed for more polar, water-soluble compounds. For this analysis, 10 mL of a water sample was



filtered (using a 0.2  $\mu\text{m}$  RC syringe filter), spiked with internal standards and analysis performed on a Waters Acquity Binary Ultra Performance Liquid Chromatograph (UPLC) (Waters Corporation, Milford, USA) coupled to a Waters Premier XE triple quadrupole mass spectrometer (LC-MS/MS) operated by MassLynx software V 4.1. The MS was operated in electrospray positive (ESI+) ionisation mode with multiple reaction monitoring (MRM). A 250  $\mu\text{L}$  aliquot was injected via an autosampler, with analyte separation performed under a MeOH/H<sub>2</sub>O (with 5 mmol/L ammonium acetate added to both phases) mobile gradient eluted through an Acquity BEH C<sub>18</sub> column (1.7  $\mu\text{m}$ , 2.1 mm  $\times$  50 mm) fitted with a VanGuard Acquity precolumn. The following compounds, including pesticides and pharmaceuticals, were qualified/quantified: chlorotoluron, isproturon, caffeine, tebuconazole, prochloraz, carbendazim, gabapentin, acetaminophen, benzotriazole, benzotriazole-methyl, ketoprofen, dimethyl-chlorotoluron, metconazole, spiroxamine, boscalid, and erythromycin. Samples were analysed separately for glyphosate and its degradation by-product, aminomethylphosphonic acid (AMPA), using LC-MS/MS. For the analysis of glyphosate and AMPA, 8 mL of a water sample was acidified to pH 1 (addition of 160  $\mu\text{L}$  of 6 M HCl) and subject to derivatisation using 9-fluorenylmethyl chloroformate using a previously published method (Ibáñez et al., 2006). Analytes were separated using the same LC-MS/MS instrument and method above. Internal standards comprised of 1,2-<sup>13</sup>C<sub>2</sub> <sup>15</sup>N Glyphosate and <sup>13</sup>C <sup>15</sup>N AMPA with a 7-point calibration with standards ranging from 0 to 2000 ng/L. Ionisation was through ESI+ (precursor ions) and MRM (product ions). LOQs were 10 ng/L for both glyphosate and AMPA with recoveries ranging from 70-130% (water spiked with internal standards).

## **Tadpole collection**

Tadpoles of *R. temporaria* were collected over a two-year period. In 2012, tadpoles were collected from CT and PF (five from each pond), and in 2013 tadpoles were collected from CT and WH (ten from each pond). Tadpoles were collected at Gosner stage 38-40, when hindlimbs were fully emerged and toes developed. Stages 30-40 are considered to be relatively stable regarding key traits, before the more dramatic changes in metamorphosis occur after stage 41 (Gosner, 1960). Tadpoles were caught using dip nets, euthanized using a solution of MS-222 (400 mg/L) buffered with sodium bicarbonate (both from Sigma Aldrich, Poole, Dorset UK) in accordance with Schedule 1 of the British Home Office Animals (Scientific Procedures) Act 1986. Tadpoles were then rinsed in distilled water and fixed immediately in the field in 70% ethanol (Fisher Scientific, UK). A small slit was made into the abdomen of each tadpole to allow the fixative to penetrate all of the tissues adequately. Ethanol was replaced after 24 hours with fresh solution. Measurements were taken of snout-to-vent length (SVL), head width (HW), body mass and tail length for all tadpoles; liver weights were also taken for tadpoles collected from CT and WH in 2013. After fixation, the following organs were excised: liver, kidney, heart, muscle, and skin, and slices (~0.5 mm thick) taken using a Stadie-Riggs tissue slicer; a technique previously employed for preparing tissue samples for spectroscopy studies (Maher et al., 2014; Obinaju et al., 2014; Taylor et al., 2011). Slices of each organ were mounted onto Low-E reflective glass slides (Kevley Technologies, Chesterland, OH, USA), dried overnight and stored in a desiccator before subsequent interrogation with ATR-FTIR spectroscopy.

## **ATR-FTIR spectroscopy**

Spectra of each sample were obtained using a Tensor 27 FTIR spectrometer with Helios ATR attachment (Bruker Optics Ltd, Coventry, UK) containing a diamond crystal ( $\approx 250 \mu\text{m} \times 250$

µm sampling area). Spectra were acquired at 8 cm<sup>-1</sup> resolution with 2× zero-filling, giving a data-spacing of 4 cm<sup>-1</sup> over the range 400-4000 cm<sup>-1</sup>. Ten-25 spectra were acquired from each sample; these were averaged in order to give a representative spectrum per organ/tadpole. Distilled water was used to clean the crystal in between analysis of each sample. A new background reading was taken prior to the analysis of each sample in order to account for changes in atmospheric conditions.

**Spectral pre-processing** Spectra were cut at the biochemical cell fingerprint region (1800-900 cm<sup>-1</sup>), baseline corrected using Savitzky-Golay (SG) 2<sup>nd</sup> order differentiation (2<sup>nd</sup> order polynomial and 9 filter coefficients), and vector normalised. Processing the data with second derivative spectroscopy allows overlapping peaks in the absorbance spectrum to be resolved, thus allowing more detailed analysis of particular peaks. By taking second derivatives, constant and linear components of baseline errors are also removed (Rieppo et al., 2012). For broad spectra the derivative intensity decreases with increasing derivative order, whereas for sharp spectra, the reverse is true. Therefore the underlying shape of the spectrum determines the intensity of the derivative spectrum, with flat peaks decreasing in intensity with each derivative order, and sharp peaks increasing in intensity, thus allowing small sharp peaks overlapped by broad flat peaks to be exposed (Kus et al.).

SG derivation is applied by fitting a simple polynomial to a small section of given size to the spectrum and calculates the derivative of the polynomial in the centre point of this section (Rinnan et al., 2009). In this study, a 2<sup>nd</sup> order polynomial and nine smoothing points were employed in the SG algorithm. This resulted in the loss of 4 wavenumbers from each end of the spectrum as a symmetric window smoothing is used requiring the number of data points on each side of the centre point to be the same, and the number of wavenumbers lost equals the number of smoothing points minus one (Rinnan et al., 2009). The polynomial order and number of smoothing points was selected based upon a compromise between noise removal

and signal distortion as no method exists which is able to eliminate all noise without losing important information. A small number of smoothing points and a high polynomial degree can give a noisy spectrum, whereas a large number of smoothing points and a low polynomial degree can distort the spectrum (Vivó-Truyols and Schoenmakers, 2006).

## **Multivariate analysis**

### **PCA**

Spectral data for each tissue were analysed using principal components analysis (PCA) for exploratory analysis. PCA is a technique which allows the large amount of data generated by IR spectroscopy to be reduced into a smaller number of principal components while retaining the majority of the variance in the data set. PCA is an unsupervised technique which looks for inherent similarities in the data and groups them the way the data ‘naturally’ cluster and is useful for small data sets (Ellis and Goodacre, 2006). PCA generates scores and loadings: scores represent each spectrum as a single data point and allow one to see if the points cluster together, suggesting similarity, or away from each other, suggesting differences. Corresponding loadings from PCA demonstrate which wavenumbers are responsible for the separation of the scores in a dataset (Trevisan et al., 2012).

After the data were mean-centred, PCA was employed to reduce the 227 absorbance values into 10 principal components (PCs), which represented > 95% of the variance in the datasets. The most statistically significant PCs were retained, as these represented the best separation in the data (see table S1 in SI for *P* values of scores for each PC for each tissue) (Malins et al., 2006; Malins et al., 2004). Loadings from the most significant PCs were used to identify wavenumbers accounting for the separation between ponds. A peak detecting algorithm was

employed to determine the five largest loadings values (constrained by a minimum of 20 cm<sup>-1</sup> spacing between values).

## **LDA**

In addition to PCA, linear discriminant analysis (LDA) was also employed to improve the discrimination between the spectra of tissues between ponds. LDA is a supervised technique (the class groupings are known *a priori*) which maximises the differences between classes, while minimising within-class heterogeneity (Martínez and Kak, 2001). For small data sets, like the ones in this study, LDA alone can over-fit the data, resulting in good data separation by chance, as the number of variables (wavenumbers) are much larger than the number of samples, therefore a data reduction technique is necessary to overcome this (Gromski et al., 2015). In this case, PCA was used prior to LDA to reduce the variables to a smaller number of PCs, which still represented ~95% of the variance in the data (see SI table S2 for the number of PCs selected for each data set). PCA also removes collinearity between variables (Gromski et al., 2015)

Data were standardised prior to the application of PCA-LDA and leave-one-out cross validation, where a small portion of the data set is used to train the model was used, again to prevent over-fitting and so as to prevent bias in the output (Trevisan et al., 2012). The output from PCA-LDA again generates scores and loading plots, however this technique generates  $n-1$  linear discriminants (LDs), which optimally separate  $n$  classes; in the case of this study a one-dimensional scores plot and one loading is generated per data set. To aid with the interpretation of the scores plots, a linear discriminant classifier (LDC) was also employed, which uses the same principle as LDA but fits a Gaussian classifier to separate the data and provides a % classification rate for each data set (Trevisan et al., 2012). Data were standardised and cross-validated as before.

## Comparison of absorbance values

Detailed quantification of differences between samples at specific wavenumbers was also implemented using absorbance values from the second derivatives; this has previously been used to quantify the biochemical entities in biological samples following analysis with vibrational spectroscopy (Rieppo et al., 2012). The second derivative has its maximum value at the same wavelength as the underlying absorbance peak, but in the opposite (negative) direction (Mark and Workman Jr, 2010).

All spectral pre-processing and data analysis was implemented using the IRootLab toolbox <https://code.google.com/p/irootlab/> (Martin et al., 2010; Trevisan et al., 2013) in Matlab (r2012a) (The MathWorks, Inc., USA), unless otherwise stated.

## Statistical analysis

Body condition indices (BCI) were calculated for each tadpole as follows:  $(\text{body mass}/\text{SVL}^3) \times 100$  (Melvin et al., 2013). Hepatosomatic indices (HSI) were also calculated for tadpoles collected from CT and WH in 2013 as follows  $(\text{liver mass}/\text{body mass}) \times 100$ .

Two-sample *t*-tests were used in order compare SVL, HW, tail length, body mass, BCI, and where indicated, liver mass and HSI between tadpoles collected from the two ponds within each year group. Tadpoles were not compared between years in order to control for the differences present due to annual factors, rather than factors due to the pond itself. Data were tested for normality and homogeneity of variances, the results of which indicated that parametric analysis was appropriate.

Two-sample *t*-tests were also used to compare absorbance values for each organ from second-derivatives between ponds within each year group and to compare the statistical significance of the scores for each PC and each LD. All statistical analyses were carried out in XL Stat (Addinsoft, Paris, France).

## **Results and discussion**

### **Water quality analysis**

Water samples were collected from March-August to cover the amphibian-breeding period and to determine water quality status given the classification of the ponds based on their land-use data. Data for the major anions and cations are presented in Table 1. Nitrate concentrations remained low (<3 mg/L) at all sites throughout the sampling period reaching the highest levels in August at CT, March at PF and April at WH. Phosphate concentrations were low at all three sites during the March sampling period (<0.08 mg/L) but were higher in April at PF and WH, at levels of 0.3 and 0.6 mg/L respectively, which are considered relatively high for UK surface waters (UKTAG, 2013; Williams et al., 2004). Phosphate levels remained high at WH during June (0.58 mg/L), coinciding with the start of metamorphosis, whereas phosphate levels were much lower at both CT and PF during this time (0.12 and 0.17 mg/L respectively).

Results from the analysis of water samples for trace organic chemicals are shown in Table 2. Screening of the water samples collected from CT, PF and WH revealed large differences in the organic contaminants detected. CT and PF appeared to be the least contaminated sites; xenobiotics detected in water samples from these sites included caffeine, several OP flame retardants and the pharmaceutical drugs acetaminophen and gabapentin, commonly found in surface waters (Mompelat et al., 2009). Both sites also had detectable levels of

336 aminomethylphosphonic acid (AMPA), the degradation product of glyphosate.

337 Aminomethylphosphonic acid may also form following the degradation of other phosphonate  
338 compounds including detergents, so is not necessarily indicative of glyphosate residue (Botta  
339 et al., 2009; Van Stempvoort et al., 2014). However, as glyphosate was also detected at PF  
340 and AMPA levels were higher here than at CT, this suggests that glyphosate was the likely  
341 source. Interestingly, relatively high levels of benzotriazole and benzotriazole-methyl were  
342 detected at CT. These compounds are commonly used as corrosion inhibitors so may have  
343 leached from farm machinery etc and they were frequently detected in a recent European-  
344 wide survey of river water (Loos et al, 2009). Water samples collected from PF also showed  
345 detectable levels of naphthalene, which has previously been associated with detrimental  
346 effects in aquatic species, although at much higher concentrations than those found in this  
347 study (Farré et al., 2008; Pillard et al., 2001).

348 Water samples collected from WH demonstrated relatively high levels of aniline, a  
349 compound generated during the degradation of several herbicides and pesticides (Xiao et al.,  
350 2007) early in the season. In contrast to CT, the other agricultural site, several pesticides,  
351 particularly fungicides were detected at WH during April and June: these included  
352 carbendazim, flusilazole, tebuconazole, boscalid, dimethachlor, chlorotoluron, metconazole  
353 and glyphosate. Carbendazim and flusilazole displayed the highest concentrations in April,  
354 with much lower levels in June and August. Glyphosate and boscalid showed the highest  
355 concentrations in June, coinciding with tadpole metamorphosis, but with much lower levels  
356 by August. Like CT, WH showed detectable levels of the corrosion inhibitors benzotriazole  
357 and benzotriazole-methyl.

358 All three sites showed detectable levels of OP flame retardants, the particular type varying  
359 between each site: TEP present at PF and WH but absent from CT; TBP only present at CT.



TCP and TCEP were detected at all three sites, with TCP generally detected at the highest levels, particularly at WH, where it reached a maximum level of 1600 ng/L, which is similar to that found in other studies, where it is the dominant OP flame retardant (van der Veen and de Boer, 2012). These compounds are frequently detected in surface waters due to their lack of biodegradability in wastewater treatment (Regnery and Püttmann, 2010) (Fries and Püttmann, 2003). As PF receives treated wastewater as well as run-off from landfill, this may explain the higher levels found here.

### Body measurements

As shown in Figure 1, tadpoles from PF (2012) were significantly larger than those from CT (2012) on all measures of body size (fig. 1A-D); tadpoles from PF also had a significantly higher BCI (fig. 1E), as determined by two sample t-tests (SVL:  $t_8 = 4.02$ ,  $P = 0.004$ ; HW:  $t_8 = 2.83$ ,  $P = 0.022$ ; tail length:  $t_8 = 4.67$ ,  $P = 0.002$ ; body mass:  $t_8 = 5.28$ ,  $P = 0.0007$ ; BCI:  $t_8 = 3.08$ ,  $P = 0.015$ ). This finding is somewhat unexpected considering that CT is regarded as the pond with better water quality. However, there were many factors not measured in this study that could account for the differences. Such factors include selection pressures such as predation/presence of competing species, population density, food availability, abiotic factors (pH, temperature and dissolved oxygen), and changes in pond depth.

In contrast, tadpoles collected from CT (2013) only differed from those collected from WH (2013) on measures of tail length and body mass (fig. 2A-E); tadpoles from CT were significantly larger on these two measures (Two sample t-test: SVL:  $t_{18} = 1.41$ ,  $P = 0.17$ ; HW:  $t_{18} = 0.57$ ,  $P = 0.57$ ; tail length:  $t_{18} = 2.40$ ,  $P = 0.027$ ; body mass:  $t_{18} = 2.22$ ,  $P = 0.04$ ; BCI:  $t_{18} = 1.16$ ,  $P = 0.26$ ). Additional measurements were made for tadpoles from CT (2013) and those from WH (2013) of liver mass and HSI (fig. 2F and 2G), with the finding that tadpoles from WH had significantly larger values of liver mass and HSI than those from CT (Two sample t-test: liver mass:  $t_{18} = 2.31$ ,  $P = 0.033$ ; LSI:  $t_{18} = 4.23$ ,  $P = 0.0005$ ). Again, the differences in

body mass and tail length could simply be due to uncontrolled factors such as food availability and pond size (Vences et al., 2002). However, the greater liver mass and HSI of tadpoles from WH in comparison to those from CT is indicative of liver inflammation or growth abnormalities (Olivares et al., 2010). Larger livers may be reflective of biochemical changes that occur as an organism attempts to maintain homeostasis and have been associated with exposure to environmental contaminants in aquatic species, including amphibians (Edwards et al., 2006; Kim et al., 2013; Lowe-Jinde and Niimi, 1984; Melvin et al., 2013; Tetreault et al., 2003). Therefore the larger HSI seen in tadpoles from WH, coupled with their smaller mass and tail length is a clear indicator of environmental stress most likely attributable to poor water quality and marked by environmental contamination through agricultural run-off at this site.

*Rana temporaria* tadpoles, like other species, are able to show developmental plasticity, where developmental rate is adjusted according to environmental conditions, producing smaller metamorphs under conditions of low food availability and high population density. Food availability and quality may also affect metamorphic performance and body size, with higher protein diets associated with a larger size at metamorphosis, (Audo et al., 1995; Beebee and Richard, 2000; Kupferberg, 1997; Álvarez and Nicieza, 2002) although this can vary with species (Casta et al., 2006). Therefore there is uncertainty regarding the effect of these uncontrolled factors and their interactions on body size parameters and a future study would aim to control such factors. Tadpoles collected in this study were at stages 38-40; a stage of development regarded as pro-metamorphic and defined as when the hindlimbs emerge and differentiate (Chambers et al., 2011; Gosner, 1960). Whilst slight differences in developmental stage can impact on size, the stages between 30-40 are considered to be one of stability in the development of key traits (Gosner, 1960). The body size of tadpoles peaks in late pro-metamorphosis before forelimb emergence (stage 42) and declines during

metamorphic climax (Álvarez and Nicieza, 2002). Therefore as the tadpoles collected in this study were at a late stage in pro-metamorphosis, but before metamorphic climax, the differences in size are unlikely to be due to this factor.

### **ATR-FTIR spectroscopy**

Figures 3A-F show the 2-dimensional scores plots and corresponding loadings following PCA for tissues which separated significantly in tadpoles collected from CT (2012) and PF (2012) (tentative assignments in table S3 in SI); 1-dimensional scores plots are shown in figures S1A-E in the SI, with corresponding statistical and classifier analysis shown in tables S4 and S5 respectively with tentative assignments in table S6. Figures 4A-E show the mean spectra for each tissue type following second derivative analysis.. Figures 5A-E show the 2-dimensional scores plots following PCA for tissues analysed from tadpoles collected from CT (2013) and WH (2013); corresponding loadings are shown in figure 6A-D (tentative assignments in table S3 in SI), with 1-dimensional scores plots following analysis with PCA-LDA shown in fig S2A-E in the SI; corresponding statistical and classifier analysis are shown in tables S4 and S5 respectively with tentative assignments in table S6. Figures 7A-E show the mean spectra for each tissue type following second derivative analysis. Table 3 shows a list of all the major second derivative peaks from each tissue and their corresponding tentative assignments. Raw spectra are shown in figures S3 and S4 in the SI.

### **Liver samples**

Results from ATR-FTIR spectroscopy demonstrated that the liver was the tissue which best-distinguished tadpoles collected from CT or PF in 2012, and also tadpoles collected from CT or WH in 2013. This is perhaps expected, as the liver is the organ responsible for metabolism of xenobiotics in vertebrates, including amphibians; therefore any changes induced by environmental contamination may be detected here (Fenoglio et al., 2011). In addition, the

liver is an energy store in tadpoles, and lipids, protein and glycogen are utilised for the completion of metamorphosis (Sheridan and Kao, 1998); thus changes in the levels of these constituents may be reflective of the energy status and thus condition of the tadpole (Melvin et al., 2013). However, other factors such as food availability and composition and predation may also impact the stress status of amphibians in synergy with chemical-insult (Relyea and Mills, 2001). This must be taken into account in the interpretation of the results and is a limitation of this study.

Comparison of liver samples from tadpoles collected from CT (2012) and those from PF (2012) demonstrated significant separation along PC1 (fig. 3A), following PCA which was associated with alterations in C-O ribose ( $991\text{ cm}^{-1}$ ), carbohydrate ( $1153\text{ cm}^{-1}$ ), Amide II ( $1516\text{ cm}^{-1}$ ), C=N cytosine ( $1601\text{ cm}^{-1}$ ) and Amide I  $\beta$ -sheets ( $1624\text{ cm}^{-1}$ ) as seen in the loadings plot in figure 3B and table S3 (SI). Further analysis with PCA-LDA led to improved separation in the scores plot (SI fig. S1A), with a correct classification rate of 99 and 90% for CT and PF respectively (see tables S4 and S5 in SI). Loadings were in regions associated with carbohydrates and proteins as before, as well as some lipid contribution (table S6 in SI). Analysis of the second derivative peak heights also showed significant differences between tadpole livers from CT (2012) and those from PF (2012) in regions associated with protein (Amide I and II), with the finding that peak heights in these regions were larger in tadpole livers from PF (2012) in comparison to those from CT (2012) (table 3, fig. 4A).

Results from PCA demonstrated that tadpole livers from CT (2013) segregated from tadpole livers from WH (2013) along PCs 1 and 4 (fig. 5A); the major loadings accounting for this separation were in regions assigned as C-O ribose, ( $988\text{-}991\text{ cm}^{-1}$ ), glycogen ( $1022\text{ cm}^{-1}$ ), symmetric phosphate stretching ( $1080\text{ cm}^{-1}$ ), Amide I ( $1616, 1624, 1639\text{ and }1697\text{ cm}^{-1}$ ) and stretching of triglycerides ( $1744\text{ cm}^{-1}$ ), as shown in fig. 6A and table S3 (SI). Supervised analysis with PCA-LDA showed an improvement in the separation of the data in the scores

plot with a high classification accuracy of 98 and 100% for CT and WH respectively, as shown in fig. S2A and table S4 in the SI. Loadings associated with this separation were again in regions assigned as carbohydrates, proteins and lipids (table S6 in SI) Analysis of the second derivative peak heights showed larger peak heights in regions associated with proteins (both Amide I and II) and symmetric phosphate stretching vibrations in tadpole livers from WH (2013) in comparison to CT (2013); however, in regions associated with lipids, peak heights were larger in tadpole livers from CT (2013) (table 3 and fig. 7A).

Lipid levels are generally low in pre-metamorphic tadpoles, rising during pro-metamorphosis, as lipids are the main energy source metabolised during metamorphic climax (Sheridan and Kao, 1998). As the tadpoles in this study were at the pro-metamorphic stage of development (emergence of hindlimbs), it was expected that a clear lipid peak would be present in the liver (figs. 4A and 7A, see SI figs. S3A and S4A). Previous studies have demonstrated changes in lipid levels in the livers of tadpoles and adult amphibians exposed to pesticides, with some reporting a decrease (Dornelles and Oliveira, 2014; Gurushankara et al., 2007), while others report an increase (Melvin et al., 2013) or no change (Zaya et al., 2011). Although no differences in hepatic lipid levels were detected between tadpoles collected in 2012 from CT and PF, tadpoles collected in 2013 from WH had significantly lower levels of hepatic lipid than those from CT in the same year. This coupled with the finding that tadpoles from WH had significantly larger livers than those from CT is suggestive of exposure to an environmental stressor, which may have resulted in the tadpoles using the lipid stored in the liver as an energy source to overcome the noxious stimuli and maintain homeostasis.

Glycogen levels may be altered in amphibian livers exposed to environmental stress due to contaminant exposure or hypoxia (Gendron et al., 1997; Loumbourdis and Kyriakopoulou-Sklavounou, 1991); levels may decrease as the organism utilises this energy source in order

to overcome the stressful situation. Results from PCA demonstrated separation between tadpole livers from CT (2012) and those from PF (2012) along PC1, with one of the largest identified loadings associated with carbohydrates including glycogen ( $1153\text{ cm}^{-1}$ ). Separation along PC4 between tadpoles from CT (2013) and those from WH (2013) also had some contribution from glycogen ( $1022\text{ cm}^{-1}$ ).

Protein levels were also found to be altered in tadpole livers collected from CT (2012) in comparison to those from PF (2012), and between tadpole livers from CT (2013) and those from WH (2013), with the finding that tadpoles from CT had lower protein levels than those from the other two sites. This is unexpected as CT is considered to have the best water quality based on the analysis conducted in this study. Reduced protein levels have previously been associated with pesticide exposure/hypoxia in amphibian livers (Dornelles and Oliveira, 2014). However, increased protein levels have also been associated with pesticide exposure in the livers of fish, with the suggestion that higher protein synthesis is initiated to compensate for protein loss, leading to a higher protein turnover (Oruç and Ünler, 1999).

#### **Muscle samples**

No significant differences were detected between tadpole muscle samples from CT (2012) and those from PF (2012) following analysis with either PCA or PCA-LDA (figs. 3C, 4B and S1B in SI). In contrast, the comparison of muscle tissue from tadpoles collected from CT (2013) and WH (2013) with PCA demonstrated separation along PC1 (fig. 5B) in regions associated with the  $\text{OCH}_3$  band of polysaccharides ( $972\text{ cm}^{-1}$ ) glycogen ( $1022\text{ cm}^{-1}$ ), C-O stretching of the phosphodiester and ribose ( $1065\text{ cm}^{-1}$ ), carbohydrates ( $1154\text{ cm}^{-1}$ ) and Amide II ( $1501\text{ cm}^{-1}$ ), as shown in the loadings plot in figure 6B and table S3 (see SI). Analysis with PCA-LDA led to some improvement in the separation of the data in the scores plot, with a reasonable classification accuracy of 71 and 80% for tadpoles from CT and WH respectively (fig. S2B and tables S4 and S5 in SI). Loadings confirmed separation based upon

changes in the phosphodiester and protein regions, with additional contributions from lipids (table S6 in SI). Second derivative peak heights show greater absorbance in muscle samples from CT (2013) in regions associated with glycogen, carbohydrates, symmetric phosphate and Amide I and II; in regions associated with asymmetric phosphate, and Amide III, peak heights were larger in tadpole muscle samples from WH (2013) (fig. 7B, table 3). Lower levels of both glycogen and protein have previously been found in muscle samples from tadpoles exposed to pesticides (Dornelles and Oliveira, 2014). Reduced glycogen levels in muscle tissues have also been associated with pesticide-induced stress in several species of fish, where glycogenolysis and glycolysis occur in order to provide more energy so that the organism can overcome stressful stimuli (Ferrando and Andreu-Moliner, 1991; Gluth and Hanke, 1985; Oruç and Üner, 1999).

#### **Other Tissues: heart, kidney and skin**

Differences between the other tissues analysed: heart, kidney and skin were small in comparison to the differences in liver and muscle tissue. Whilst analysis with PCA showed no significant differences between hearts from tadpoles collected from CT (2012) and those from PF (2012) (fig. 3D), the use of PCA-LDA led to an improvement in data separation, as shown in fig. S1C, and tables S4 and S5 in the SI. The largest loadings values accounting for the separation were in regions associated with symmetric phosphate stretching vibrations ( $1088\text{ cm}^{-1}$ ) as well as carbohydrates ( $1138\text{ cm}^{-1}$ ) and collagen ( $1196\text{ cm}^{-1}$ ), as shown in table S6 (SI). Analysis of the second derivative peak heights revealed a significant difference at the peak associated with asymmetric phosphate stretching; where it was larger at CT (2012) than PF (2012) as shown in figure 4C. Tadpole hearts collected from CT (2013) and WH (2013) demonstrated some separation along PC3 following PCA (fig. 5C), but this was not statistically significant ( $P=0.06$ ); however a significant improvement in data separation was seen when PCA-LDA was employed, with a classification accuracy of 76 and 71% for

tadpoles from CT and WH respectively (fig S2C and table S4 and S5 in SI) Loadings values confirmed the separation in regions assigned as collagen and protein (amide I) as shown in table S6 (SI). Analysis of the second derivative peak heights demonstrated significant differences between CT (2013) and WH (2013) in the region associated with CH<sub>3</sub> bending of lipids, where peak height was smaller at CT than WH, and in the Amide I region, where the peak height was larger at CT in comparison to WH (fig 7C, table 3). Previous work in fish has also shown differences in heart tissue in fish collected from polluted rivers, in regions associated with Amide I and lipids, as measured with ATR-FTIR spectroscopy (Obinaju et al., 2014). Whilst no previous spectroscopic measurements of tadpole hearts have been published, it is known that cardiac output in tadpoles may be altered in response to stressful situations induced by xenobiotics (Costa et al., 2008). Future work could attempt to correlate differences in cardiac output with the spectral signature.

No significant differences were found in the spectral signature of tadpole kidney samples collected from CT (2012) or PF (2012) when analysed with either PCA or PCA-LDA (figs. 3E and 4D, fig. S1D in SI). However, PCA revealed significant separation between kidney samples from tadpoles from CT (2013) and those from WH (2013) as shown in fig. 5D. Loadings from PCA revealed that these differences were attributable to protein (Amide I and II) and lipid alterations (fig. 6C, see SI table S2). Analysis with PCA-LDA actually led to poorer data separation, as shown in fig S2D and tables S4 and S4 in the SI which may occur when working with small data sets, as in this study (Martínez and Kak, 2001). Second derivative peak analysis also confirmed alterations associated with Amide I/stretching of fatty acids at 1670 cm<sup>-1</sup>, with kidney samples from CT having a larger peak height than those from WH (fig 7D, table 3). The kidney, like the liver is susceptible to the effects of several toxicants, with a previous study in amphibians finding differences in the structure and histochemistry of kidney samples from adult frogs collected from polluted compared to



unpolluted sites (Fenoglio et al., 2011). Alterations in the kidneys of fish from polluted sites have previously been detected using ATR-FTIR spectroscopy; these were also in regions associated with Amide I and II of proteins, as in this study; however, no alterations in lipids were detected, in contrast to that found in this study (Obinaju et al., 2014).

There were no differences detected in the tadpole skin samples from CT (2012) in comparison to those from PF (2012) when the data were analysed with PCA, PCA-LDA or using the peak absorbances (fig. 3F and 4E, table 3, fig. S1E; tables S4 and S5 in SI). In contrast, skin samples taken from tadpoles from CT (2013) and WH (2013) showed some separation along PC3 following PCA (fig. 5E); this was mainly in regions associated with Amide I ( $1616, 1640\text{ cm}^{-1}$ ), with some contribution from lipids ( $1497, 1694\text{ cm}^{-1}$ ), as shown in the loadings plot in figure 6D and table S3 (see SI). The use of PCA-LDA led to improved data separation as shown in the scores plot in fig S2E and tables S4 and S5, associated with amide I proteins as before, with some contributions from collagen and C-O stretching of carbohydrates (table S6 in SI). Analysis of second derivative peak heights showed no significant differences between skin samples from CT (2013) and WH (2013) (fig. 7E, table 3). That some separation was apparent between skin samples is of note, given that the skin is the first organ that environmental contaminants come into contact with in amphibian species. The skin of amphibians is permeable to water, where it plays a vital role in respiration and osmoregulation; therefore the skin provides a significant exposure route to chemicals in addition to that from ingestion and has previously been proposed as a bioindicator of deleterious environmental conditions, with structural changes detected following exposure to environmental contaminants (Bernabò et al., 2013; Fenoglio et al., 2009; Fenoglio et al., 2006; Haslam et al., 2014). The skin of larval amphibians may also be more susceptible to chemical insult than that of adults due to the lack of specialised cells and many of the detoxifying enzymes, which are present in adults (Fenoglio et al., 2009).

## Conclusions

ATR-FTIR spectroscopy is capable of detecting differences in a range of tissue samples from tadpoles of the Common frog collected from ponds with varying water quality and different types of environmental contamination. Interestingly, despite the unexpected finding that tadpoles from the urban pond were on average larger than those from the rural pesticide-free agricultural pond, the differences in tissues detected by ATR-FTIR spectroscopy were relatively small and mainly found in the liver. In contrast, the differences between tadpoles from the rural pesticide-free agricultural and pesticide-impacted agricultural pond were detected in multiple tissues, most notably the liver and muscle.

The liver was the organ which consistently distinguished tadpoles collected from the relatively unpolluted agricultural pond, and ponds with pollutants associated with urban and agricultural activity. Tadpoles collected from the pesticide-impacted agricultural pond also had relatively larger livers and reduced lipid levels; a finding associated with exposure to environmental contaminants such as pesticides and other trace organic pollutants, although the effect of raised nutrient levels (such as nitrate and phosphate), possibly in synergy with other pollutants, needs to be investigated. Interactions with other factors such as food availability and predation may also affect these parameters; therefore any future study would attempt to control these conditions. Clear differences were also apparent in the muscle tissue of tadpoles from a pond with no pesticide input and those from a pond impacted by several pesticides. This finding was also apparent to a lesser extent in the kidney, heart and skin of these tadpoles.

This study is the first to characterise a range of tissues from an amphibian species with ATR-FTIR spectroscopy. Additionally, this study demonstrates the possible use of this technique as a rapid and cost-effective environmental monitoring tool. This technology could be of

608 great promise as an early warning for assessing the health of amphibian populations exposed  
609 to varying or diminished water quality.

610

611 **Acknowledgements** The Doctoral programme of RS was funded by a NERC-CEH CASE  
612 studentship. The authors wish to thank Professor John Quinton (LEC) and the respective  
613 farmers and landowners for access to CT and WH experimental ponds, funded by the UK  
614 Department of Environment, Food and Rural Affairs (DEFRA), under the project ‘Mitigation  
615 of Phosphorus and Sediment 2 (MOPS-2)’, contract WQ0127. Permission to sample at  
616 Pennington Flash was granted by Wigan and Leigh Culture Trust.

617

## Figure headings

**Figure 1.** Comparison of body size parameters of pro-metamorphic *Rana temporaria* tadpoles collected in 2012 from CT: a rural agricultural pond with no pesticide input and PF: an urban pond impacted by wastewater and landfill run-off. Measurements are snout-vent-length (SVL), (A), head width (HW), (B), tail length, (C), body mass, (D) and body condition index (BCI), (E). Two-sample *t*-tests were used to compare each body size parameter. Different letters denote a significant difference ( $P < 0.05$ ).

**Figure 2.** Comparison of body size parameters of pro-metamorphic *Rana temporaria* tadpoles collected in 2013 from a CT: a rural agricultural pond with no pesticide input and WH: an agricultural pond known to be impacted by pesticides. Measurements are snout-vent-length (SVL), (A), head width (HW), (B), tail length, (C), body mass, (D), body condition index (BCI), (E), liver mass (F), and hepatosomatic index (HSI), (G). Two-sample *t*-tests were used to compare each body size parameter. Different letters denote a significant difference ( $P < 0.05$ ).

**Figure 3.** Two-dimensional scores plots and significant loadings following principal components analysis (PCA) of ATR-FTIR spectra obtained from several different tissues taken from *Rana temporaria* pro-metamorphic tadpoles. Tissues are liver (A: scores, B: loadings), muscle (B), heart (C), kidney (D) and skin (E). Tadpoles were collected in 2012 from CT: a rural agricultural pond with no pesticide input or PF: an urban pond impacted by wastewater and landfill run-off ( $n = 10$ ). Two sample *t*-tests were employed to detect differences in the PC scores between ponds within each year. Asterisks indicate a *P* value of  $< 0.05$  (\*) or  $< 0.01$  (\*\*). Values in parentheses show the contribution of each principal component to the overall variance.

**Figure 4.** Second derivative mean spectra of tissues taken from *Rana temporaria* pro-metamorphic tadpoles. Spectra were cut at the biochemical fingerprint region (1800-900 cm<sup>-1</sup>), processed with Savitzky-Golay second-order differentiation and vector-normalised. Tissues are liver (**A**), muscle (**B**), heart (**C**), kidney (**D**) and skin (**E**). Tadpoles were collected in 2012, from CT: a rural agricultural pond with no pesticide input or PF: an urban pond impacted by wastewater and landfill run-off ( $n = 10$ ). Peaks are labelled with the corresponding wavenumbers. Two sample *t*-tests were employed to detect differences in the second derivative peak height at each labelled peak between ponds within each year. Asterisks indicate a *P* value of < 0.05 (\*) or < 0.01 (\*\*).

**Figure 5.** Two-dimensional scores plots following principal components analysis (PCA) of ATR-FTIR spectra obtained from several different tissues taken from *Rana temporaria* pro-metamorphic tadpoles. Tissues are liver (**A**), muscle (**B**), heart (**C**), kidney (**D**) and skin (**E**). Tadpoles were collected in 2013 from CT: a rural agricultural pond with no pesticide input or WH: an agricultural pond known to be impacted by pesticides ( $n = 20$ ). Two sample *t*-tests were employed to detect differences in the PC scores between ponds within each year. Asterisks indicate a *P* value of < 0.05 (\*) or < 0.01 (\*\*). Values in parentheses show the contribution of each principal component to the overall variance.

**Figure 6.** Loadings plots following PCA of ATR-FTIR spectra obtained from several different tissues taken from *Rana temporaria* pro-metamorphic tadpoles. **A:** Liver; **B:** Muscle; **C:** Kidney; **D:** Skin. Ponds are as follows: CT: a rural agricultural pond with no pesticide input; WH: an agricultural pond known to be impacted by pesticides.

**Figure 7.** Second derivative mean spectra of tissues taken from *Rana temporaria* pro-metamorphic tadpoles. Spectra were cut at the biochemical fingerprint region (1800-900 cm<sup>-1</sup>), processed with Savitzky-Golay second-order differentiation and vector-normalised.

665 Tissues are liver (**A**), muscle (**B**), heart (**C**), kidney (**D**) and skin (**E**). Tadpoles were collected  
666 in 2013, from CT: a rural agricultural pond with no pesticide input or WH: an agricultural  
667 pond known to be impacted by pesticides ( $n = 20$ ). Peaks are labelled with the corresponding  
668 wavenumbers. Two sample  $t$ -tests were employed to detect differences in the second  
669 derivative peak height at each labelled peak between ponds within each year. Asterisks  
670 indicate a  $P$  value of  $< 0.05$  (\*) or  $< 0.01$  (\*\*).

671

672

**Table 1. Analysis of water samples for inorganic anions and cations collected from CT: a rural agricultural pond with no pesticide input; WH: an agricultural pond known to be impacted by pesticides and PF: an urban pond impacted by wastewater and landfill run-off. Water samples were collected during the breeding season of *Rana temporaria* (March-August). Values marked < LD were below limit of detection.**

<b>Anion/Cation (mg/L)</b>	<b>CT March</b>	<b>CT April</b>	<b>CT June</b>	<b>CT August</b>	<b>PF March</b>	<b>PF April</b>	<b>PF June</b>	<b>WH March</b>	<b>WH April</b>	<b>WH June</b>	<b>WH August</b>
<b>Al</b>	< LD	< LD	< LD	< LD	< LD	< LD	< LD	< LD	< LD	< LD	< LD
<b>Ca</b>	84.4	77.6	64.8	105	46.3	36.8	30.7	53.2	56.6	33.3	47.9
<b>Cl</b>	9.06	10.4	2.98	8.44	21.6	11.6	11.4	64.1	47.8	36.1	15.1
<b>Fe</b>	0.47	0.007	0.019	0.014	0.008	0.76	0.095	0.026	0.03	0.15	0.016
<b>K</b>	1.97	1.57	0.507	0.811	3.88	4.01	5.27	11.3	18.1	11.5	10.4
<b>Mg</b>	2.95	4.37	5.09	4.74	10.0	7.99	6.00	9.35	10.7	5.54	8.96
<b>Na</b>	4.88	4.97	3.03	4.95	15.0	9.82	9.27	38.8	37.2	24.6	12.6
<b>NH<sub>4</sub>-N</b>	0.028	0.412	1.47	0.014	0.06	0.128	1.28	0.303	0.282	5.50	0.033
<b>NO<sub>3</sub>-N</b>	< 0.001	0.219	0.012	1.62	0.427	1.18	0.016	0.01	2.49	0.017	0.912
<b>PO<sub>4</sub>-P</b>	0.029	0.033	0.121	0.15	0.068	0.304	0.17	0.006	0.639	0.584	0.089
<b>SO<sub>4</sub>-S</b>	0.706	0.195	0.124	0.225	6.59	2.61	1.30	9.92	12.7	2.70	11.6

**Table 2. Organic contaminant analysis of water samples collected from CT: a rural agricultural pond with no pesticide input; WH: an agricultural pond known to be impacted by pesticides and PF: an urban pond impacted by wastewater and landfill run-off. Water samples were collected to coincide with the breeding season of *Rana temporaria* (March-August). Values marked < LD were below limit of detection.**

<b>Chemical (ng/L)</b>	<b>CT Mar</b>	<b>CT Apr</b>	<b>CT Jun</b>	<b>CT Aug</b>	<b>PF Mar</b>	<b>PF Apr</b>	<b>WH Mar</b>	<b>WH Apr</b>	<b>WH Jun</b>	<b>WH Aug</b>
Naphthalene	<LD	<LD	<LD	<LD	10	<LD	<LD	<LD	<LD	<LD
Aniline	<LD	<LD	<LD	<LD	<LD	<LD	1100	<LD	<LD	<LD
Dimethachlor	<LD	<LD	<LD	<LD	<LD	<LD	<LD	26	49	<LD
Chlorotoluron	<LD	<LD	<LD	<LD	<LD	<LD	<LD	23	52	<LD
Caffeine	<LD	441	<LD	<LD	<LD	107	<LD	<LD	200	103
Glyphosate	<LD	<LD	<LD	<LD	40	<LD	<LD	50	2310	50
AMPA	<LD	150	<LD	45	130	658	<LD	1470	1040	39
Tebuconazole	<LD	<LD	<LD	<LD	<LD	<LD	76	<LD	34	109
Carbendazim	<LD	<LD	<LD	<LD	<LD	<LD	<LD	866	76	<LD
TEP	<LD	<LD	<LD	<LD	11	11	<LD	<LD	160	<LD
TBP	<LD	13	<LD	<LD	<LD	<LD	<LD	<LD	<LD	<LD



TCEP	<LD	26	<LD	<LD	190	12	<LD	7.2	42	5.7
TCPP	15	125	<LD	20	142	314	25	1600	539	187
Flusilazole	<LD	<LD	<LD	<LD	<LD	<LD	<LD	552	30	26
Gabapentin	<LD	<LD	23	25	75	<LD	21	<LD	56	<LD
Acetaminophen	<LD	<LD	34	35	20	<LD	50	33	41	29
Benzotriazole	<LD	<LD	<LD	<LD	<LD	<LD	<LD	85	206	47
Benzotriazole-methyl	<LD	<LD	1520	53	<LD	<LD	<LD	268	263	60
Ketoprofen	<LD	<LD	<LD	<LD	<LD	<LD	<LD	<LD	13	<LD
Desmethyl-chlrotoluron	<LD	<LD	<LD	35	<LD	<LD	<LD	<LD	<LD	<LD
Metconazole	<LD	<LD	<LD	<LD	<LD	<LD	<LD	<LD	14	<LD
Spiroxamin	<LD	<LD	<LD	<LD	<LD	<LD	30	<LD	<LD	<LD
Boscalid	<LD	<LD	<LD	<LD	<LD	<LD	<LD	<LD	122	19
Erythromycin	<LD	<LD	<LD	<LD	<LD	<LD	<LD	181	24	<LD

**Table 3. Wavenumbers and assigned bands of infrared peaks following ATR-FTIR analysis of several organs of pro-metamorphic *Rana temporaria* tadpoles. Absorbance values of second derivatives were compared between CT: a rural agricultural pond with no pesticide input and PF: an urban pond impacted by wastewater and landfill run-off in 2012 and between CT and WH: an agricultural pond known to be impacted by pesticides in 2013.**

<b>Tissue</b>	<b>Wavenumber (cm<sup>-1</sup>)</b>	<b>Proposed Assignment <sup>a</sup></b>	<b>CT vs. PF (2012)</b>	<b>CT vs. WH (2013)</b>
<b>Liver</b>	991	C-O ribose <sup>1</sup>	NS	CT < WH *
	1018	Glycogen <sup>1</sup>	NS	NS
	1080	PO <sub>2</sub> - symmetric stretching: nucleic acids and phospholipids <sup>2, 3</sup>	NS	CT < WH **
		C-O stretch: glycogen <sup>2, 3</sup>		
	1111	$\nu(\text{CO})$ , $\nu(\text{CC})$ ring (polysaccharides, cellulose) <sup>1</sup>	NS	NS
	1150	CO-O-C asymmetric stretching: glycogen and nucleic acids <sup>2, 3</sup>	NS	NS
	1238	PO <sub>2</sub> - asymmetric stretch: mainly nucleic acids with the little contribution from phospholipids <sup>2, 3</sup>	NS	CT < WH *
	1335	$\delta(\text{CH})$ , ring (polysaccharides, pectin)	NS	CT < WH **
	1373	Deformation N-H, C-H <sup>1</sup>	NS	CT > WH **
	1412	COO symmetric stretch: fatty acids and amino acids <sup>4</sup>	NS	NS
	1462	CH <sub>2</sub> bending of lipids <sup>2, 3</sup>	NS	CT > WH **
	1516	Amide II <sup>1</sup>	NS	CT < WH **

	1531	Amide II <sup>1</sup>	CT < PF **	CT < WH **
	1624	Amide I $\beta$ -sheets <sup>5</sup>	CT < PF **	CT < WH **
	1651	Amide I protein $\alpha$ -helix <sup>2, 3, 5</sup>	CT < PF *	NS
	1744	Ester C-O stretch: triglycerides, cholesterol esters <sup>2, 3</sup>	NS	CT > WH **
<b>Muscle</b>	995	C-O ribose, C-C <sup>1</sup>	NS	CT > WH**
	1026	Glycogen <sup>1</sup>	NS	CT > WH **
	1080	PO <sub>2</sub> <sup>-</sup> symmetric stretch: nucleic acids and phospholipids C-O stretch: glycogen <sup>6</sup>	NS	CT > WH **
	1115	Symmetric stretching P-O-C <sup>1</sup>	NS	NS
	1157	C-O stretching of protein and carbohydrates <sub>1</sub>	NS	CT > WH **
	1235	PO <sub>2</sub> <sup>-</sup> asymmetric stretch: mainly nucleic acids with little contribution from phospholipids <sup>6</sup>	NS	CT < WH *
	1312	Amide III of proteins <sup>1</sup>	NS	CT < WH *
	1393	COO <sup>-</sup> symmetric stretch: fatty acids and amino acids <sup>6</sup>	NS	CT < WH *
	1447	CH <sub>2</sub> bending mainly lipids <sup>6</sup>	NS	NS
	1512	Amide II, C-H bending <sup>1</sup>	NS	CT < WH *
	1532	Amide II stretching C=N, C=C <sup>1</sup>	NS	CT > WH *
	1624	Amide I $\beta$ -sheets <sup>5</sup>	NS	NS

	1647	Amide I <sup>1</sup>	NS	CT > WH *
	1670	Amide I (anti-parallel $\beta$ -sheet) $\nu(\text{C}=\text{C})$ trans, lipids, fatty acids <sup>1</sup>	NS	NS
	1690	Peak of nucleic acid due to ring breathing mode and base carbonyl stretching <sup>1</sup>	NS	NS
	1744	C=O stretching lipids <sup>1,4</sup>	NS	NS
<b>Heart</b>	964	C-O deoxyribose, C-C <sup>1</sup>	NS	NS
	1026	Glycogen <sup>1</sup>	NS	NS
	1053	$\nu$ C-O and $\delta$ C-O of carbohydrates <sup>1</sup>	NS	NS
	1080	PO <sub>2</sub> <sup>-</sup> symmetric stretching: nucleic acids and phospholipids <sup>7</sup>	NS	NS
		C-O stretch: glycogen <sup>2,3</sup>		
	1115	Symmetric stretching P-O-C <sup>1</sup>	NS	NS
	1161	C-O asymmetric stretching of glycogen <sup>7,8</sup>	NS	NS
	1231	PO <sub>2</sub> <sup>-</sup> asymmetric stretching: phospholipids, nucleic acids <sup>2</sup>	CT > PF *	NS
	1312	Amide III band of proteins <sup>1</sup>	NS	NS
	1389	CH <sub>3</sub> bending: lipids <sup>7</sup>	NS	CT < WH **
	1447	CH <sub>2</sub> bending mainly lipids <sup>6</sup>	NS	NS
	1512	Amide II, C-H bending <sup>1</sup>	NS	NS

	1624	Amide I $\beta$ -sheets <sup>5</sup>	NS	NS
	1643	Amide I, C=O stretching vibrations <sup>1</sup>	NS	NS
	1670	Amide I (anti-parallel $\beta$ -sheet) $\nu$ (C=C) trans, lipids, fatty acids <sup>1</sup>	NS	CT > WH **
	1690	Peak of nucleic acid due to ring breathing mode and base carbonyl stretching <sup>1</sup>	NS	NS
	1744	C=O stretching lipids <sup>1,4</sup>	NS	NS
<b>Kidney</b>	964	C-O deoxyribose, C-C <sup>1</sup>	NS	NS
	1026	Glycogen <sup>1</sup>	NS	NS
	1057	C-O stretching, polysaccharides <sup>8</sup>	NS	NS
	1080	PO <sub>2</sub> - symmetric stretching of nucleic acids	NS	NS
	1115	Symmetric stretching P-O-C <sup>1</sup>	NS	NS
	1161	C-O asymmetric stretching of glycogen <sup>8</sup>	NS	NS
	1231	PO <sub>2</sub> - asymmetric stretching of mainly phospholipids <sup>8</sup>	NS	NS
	1312	Amide III band of proteins <sup>1</sup>	NS	NS
	1393	COO <sup>-</sup> symmetric stretch of fatty acids and amino acids <sup>8</sup>	NS	NS
	1447	Asymmetric CH <sub>3</sub> bending of the methyl groups of proteins <sup>1</sup>	NS	NS
	1516	Amide II <sup>1</sup>	NS	NS

	1532	Amide II stretching C=N, C=C	NS	NS
	1624	Amide I $\beta$ -sheets <sup>5</sup>	NS	NS
	1647	Amide I <sup>1</sup>	NS	NS
	1670	Amide I (anti-parallel $\beta$ -sheet)	NS	CT > WH *
		$\nu$ (C=C) trans, lipids, fatty acids <sup>1</sup>		
	1690	Peak of nucleic acid due to ring breathing mode and base carbonyl stretching <sup>1</sup>	NS	NS
	1744	C=O stretching of lipids <sup>1</sup>	NS	NS
<b>Skin</b>	964	C-O deoxyribose, C-C <sup>1</sup>	NS	NS
	1030	Collagen <sup>1</sup>	NS	NS
		$\nu$ (CC), lipid cis <sup>9</sup>		
	1080	$\nu$ (CC), lipid trans <sup>9</sup>	NS	NS
	1119	$\nu$ (CC), lipid trans <sup>9</sup>	NS	NS
	1165	$\nu$ (CC), $\delta$ (COH) <sup>9</sup>	NS	NS
	1231	Amide III protein <sup>1, 10</sup>	NS	NS
	1312	Amide II protein <sup>1</sup>	NS	NS
	1393	$\delta$ [C(CH <sub>3</sub> ) <sub>2</sub> ] symmetric <sup>1,9</sup>	NS	NS
	1447	$\delta$ [C(CH <sub>3</sub> ) <sub>2</sub> ] symmetric <sup>1</sup>	NS	NS
	1512	Amide II <sup>1</sup>	NS	NS
	1543	Amide II <sup>1</sup>	NS	NS

1624	$\nu(\text{C=O})$ , amide I, $\beta$ <sup>9</sup>	NS	NS
1643	Collagen <sup>10</sup>	NS	NS
	$\nu(\text{C=O})$ , amide I, $\alpha$ <sup>9</sup>		
1690	Amide I <sup>1</sup>	NS	NS
1744	Lipid <sup>1</sup>	NS	NS

$\nu$ : stretching;  $\delta$ : deformation

<sup>a</sup> Sources 1. Movasaghi et al. (2008) 2. Cakmak et al. (2003) 3. Cakmak et al. (2006) 4. Abdel-Gawad et al. (2012) 5. Palaniappan et al. (2011) 6. Palaniappan et al. (2008) 7. Toyran et al. (2006) 8. Palaniappan et al. (2009). 9. Greve et al. 2008 10. Purna Sai et al. (2001).

Asterisks denote significance at the  $P < 0.05$  level (\*), and  $P < 0.01$  level (\*\*). NS = not significant.

## References

- Abdel-Gawad, F.K., Ibrahim, H.S., Ammar, N.S., Ibrahim, M., 2012. Spectroscopic analyses of pollutants in water, sediment and fish. *Spectrochimica Acta Part A: Molecular and Biomolecular Spectroscopy* 97, 771-777.
- Altwegg, R., Reyer, H.-U., 2003. Patterns of natural selection on size at metamorphosis in water frogs. *Evolution* 57, 872-882.
- Audo, M.C., Mann, T.M., Polk, T.L., Loudenslager, C.M., Diehl, W.J., Altig, R., 1995. Food deprivation during different periods of tadpole (*Hyla chrysoscelis*) ontogeny affects metamorphic performance differently. *Oecologia* 103, 518-522.
- Baker, M.J., Trevisan, J., Bassan, P., Bhargava, R., Butler, H.J., Dorling, K.M., Fielden, P.R., Fogarty, S.W., Fullwood, N.J., Heys, K.A., Hughes, C., Lasch, P., Martin-Hirsch, P.L., Obinaju, B., Sockalingum, G.D., Sulé-Suso, J., Strong, R.J., Walsh, M.J., Wood, B.R., Gardner, P., Martin, F.L., 2014. Using Fourier transform IR spectroscopy to analyze biological materials. *Nature Protocols* 9, 1771-1791.
- Beebee, T.J.C., Griffiths, R.A., 2005. The amphibian decline crisis: a watershed for conservation biology? *Biological Conservation* 125, 271-285.
- Beebee, T.J.C., Richard, G., 2000. *Amphibians and reptiles*. Collins London (UK).
- Bellisola, G., Sorio, C., 2012. Infrared spectroscopy and microscopy in cancer research and diagnosis. *American Journal of Cancer Research* 2, 1.
- Bernabò, I., Guardia, A., La Russa, D., Madeo, G., Tripepi, S., Brunelli, E., 2013. Exposure and post-exposure effects of endosulfan on *Bufo bufo* tadpoles: Morpho-histological and ultrastructural study on epidermis and iNOS localization. *Aquatic Toxicology* 142-143, 164-175.
- Blaustein, A.R., Han, B.A., Relyea, R.A., Johnson, P.T.J., Buck, J.C., Gervasi, S.S., Kats, L.B., 2011. The complexity of amphibian population declines: understanding the role of cofactors in driving amphibian losses, in: Ostfeld, R.S., Schlesinger, W.H. (Eds.), *Year in Ecology and Conservation Biology*, pp. 108-119.
- Blaustein, A.R., Romansic, J.M., Kiesecker, J.M., Hatch, A.C., 2003. Ultraviolet radiation, toxic chemicals and amphibian population declines. *Diversity and Distributions* 9, 123-140.
- Blaustein, A.R., Wake, D.B., 1995. The puzzle of declining amphibian populations. *Scientific American* 272, 52-57.
- Botta, F., Lavison, G., Couturier, G., Alliot, F., Moreau-Guigon, E., Fauchon, N., Guery, B., Chevreuil, M., Blanchoud, H., 2009. Transfer of glyphosate and its degradate AMPA to surface waters through urban sewerage systems. *Chemosphere* 77, 133-139.
- Bridges, C.M., 2000. Long-term effects of pesticide exposure at various life stages of the Southern Leopard frog (*Rana sphenoccephala*). *Archives of Environmental Contamination and Toxicology* 39, 91-96.
- Cakmak, G., Togan, I., Severcan, F., 2006. 17 $\beta$ -Estradiol induced compositional, structural and functional changes in rainbow trout liver, revealed by FT-IR spectroscopy: a comparative study with nonylphenol. *Aquatic Toxicology* 77, 53-63.
- Cakmak, G., Togan, I., Uğuz, C., Severcan, F., 2003. FT-IR spectroscopic analysis of rainbow trout liver exposed to nonylphenol. *Applied Spectroscopy* 57, 835-841.
- Casta, xf, eda, L., xa, E, Sabat, P., Gonzalez, S., P, Nespolo, R., F, 2006. Digestive Plasticity in Tadpoles of the Chilean Giant Frog (*Caudiverbera caudiverbera*): Factorial Effects of Diet and Temperature. *Physiological and Biochemical Zoology: Ecological and Evolutionary Approaches* 79, 919-926.
- Chambers, D.L., Wojdak, J.M., Du, P., Belden, L.K., 2011. Corticosterone Level Changes throughout Larval Development in the Amphibians *Rana sylvatica* and *Ambystoma jeffersonianum* Reared under Laboratory, Mesocosm, or Free-living Conditions. *Copeia* 2011, 530-538.
- Corte, L., Rellini, P., Roscini, L., Fatichenti, F., Cardinali, G., 2010. Development of a novel, FTIR (Fourier transform infrared spectroscopy) based, yeast bioassay for toxicity testing and stress response study. *Analytica Chimica Acta* 659, 258-265.



Costa, M.J., Monteiro, D.A., Oliveira-Neto, A.L., Rantin, F.T., Kalinin, A.L., 2008. Oxidative stress biomarkers and heart function in bullfrog tadpoles exposed to Roundup Original®. *Ecotoxicology* 17, 153-163.

Dornelles, M.F., Oliveira, G.T., 2014. Effect of atrazine, glyphosate and quinclorac on biochemical parameters, lipid peroxidation and survival in bullfrog tadpoles (*Lithobates catesbeianus*). *Archives of Environmental Contamination and Toxicology* 66, 415-429.

Edwards, T.M., McCoy, K.A., Barbeau, T., McCoy, M.W., Thro, J.M., Guillette, L.J., 2006. Environmental context determines nitrate toxicity in Southern toad (*Bufo terrestris*) tadpoles. *Aquatic Toxicology* 78, 50-58.

Egea-Serrano, A., Relyea, R.A., Tejedo, M., Torralva, M., 2012. Understanding of the impact of chemicals on amphibians: a meta-analytic review. *Ecology and Evolution* 2, 1382-1397.

Ellis, D.I., Goodacre, R., 2006. Metabolic fingerprinting in disease diagnosis: biomedical applications of infrared and Raman spectroscopy. *Analyst* 131, 875-885.

Farré, M.I., Pérez, S., Kantiani, L., Barceló, D., 2008. Fate and toxicity of emerging pollutants, their metabolites and transformation products in the aquatic environment. *TrAC Trends in Analytical Chemistry* 27, 991-1007.

Fenoglio, C., Albicini, F., Milanesi, G., Barni, S., 2011. Response of renal parenchyma and interstitium of *Rana* snk. *esculenta* to environmental pollution. *Ecotoxicology and Environmental Safety* 74, 1381-1390.

Fenoglio, C., Grosso, A., Boncompagni, E., Gandini, C., Milanesi, G., Barni, S., 2009. Exposure to heptachlor: Evaluation of the effects on the larval and adult epidermis of *Rana* kl. *esculenta*. *Aquatic Toxicology* 91, 151-160.

Fenoglio, C., Grosso, A., Boncompagni, E., Milanesi, G., Gandini, C., Barni, S., 2006. Morphofunctional evidence of changes in principal and mitochondria-rich cells in the epidermis of the frog *Rana* kl. *esculenta* living in a polluted habitat. *Archives of Environmental Contamination and Toxicology* 51, 690-702.

Ferrando, M.D., Andreu-Moliner, E., 1991. Effects of lindane on fish carbohydrate metabolism. *Ecotoxicology and Environmental Safety* 22, 17-23.

Fries, E., Puttmann, W., 2003. Monitoring of the three organophosphate esters TBP, TCEP and TBEP in river water and ground water (Oder, Germany). *Journal of Environmental Monitoring* 5, 346-352.

Gendron, A.D., Bishop, C.A., Fortin, R., Hontela, A., 1997. In vivo testing of the functional integrity of the corticosterone-producing axis in mudpuppy (amphibia) exposed to chlorinated hydrocarbons in the wild. *Environmental Toxicology and Chemistry* 16, 1694-1706.

Gluth, G., Hanke, W., 1985. A comparison of physiological changes in carp, *Cyprinus carpio*, induced by several pollutants at sublethal concentrations: I. The dependency on exposure time. *Ecotoxicology and Environmental Safety* 9, 179-188.

Gosner, K.L., 1960. A simplified table for staging anuran embryos and larvae with notes on identification. *Herpetologica* 16, 183-190.

Greulich, K., Pflugmacher, S., 2003. Differences in susceptibility of various life stages of amphibians to pesticide exposure. *Aquatic Toxicology* 65, 329-336.

Greve, T.M., Andersen, K.B., Nielsen, O.F., 2008. ATR-FTIR, FT-NIR and near-FT-Raman spectroscopic studies of molecular composition in human skin in vivo and pig ear skin in vitro. *Spectroscopy: An International Journal* 22, 437-457.

Gromski, P.S., Muhamadali, H., Ellis, D.I., Xu, Y., Correa, E., Turner, M.L., Goodacre, R., 2015. A tutorial review: Metabolomics and partial least squares-discriminant analysis—a marriage of convenience or a shotgun wedding. *Analytica chimica acta* 879, 10-23.

Gurushankara, H.P., Meenakumari, D., Krishnamurthy, S.V., Vasudev, V., 2007. Impact of malathion stress on lipid metabolism in *Limnonectes limnocharis*. *Pesticide Biochemistry and Physiology* 88, 50-56.

Haslam, I.S., Roubos, E.W., Mangoni, M.L., Yoshizato, K., Vaudry, H., Kloepper, J.E., Pattwell, D.M., Maderson, P.F.A., Paus, R., 2014. From frog integument to human skin: dermatological perspectives from frog skin biology. *Biological Reviews* 89, 618-655.

Hayes, T.B., Case, P., Chui, S., Chung, D., Haeffele, C., Haston, K., Lee, M., Mai, V.P., Marjuoa, Y., Parker, J., Tsui, M., 2006. Pesticide mixtures, endocrine disruption, and amphibian declines: Are we underestimating the impact? *Environmental Health Perspectives* 114, 40-50.

Henczova, M., Deer, A.K., Filla, A., Komlosi, V., Mink, J., 2008. Effects of Cu<sup>2+</sup> and Pb<sup>2+</sup> on different fish species: Liver cytochrome P450-dependent monooxygenase activities and FTIR spectra. *Comparative Biochemistry and Physiology C-Toxicology & Pharmacology* 148, 53-60.

Holman, H.-Y.N., Goth-Goldstein, R., Martin, M.C., Russell, M.L., McKinney, W.R., 2000. Low-dose responses to 2, 3, 7, 8-tetrachlorodibenzo-p-dioxin in single living human cells measured by synchrotron infrared spectromicroscopy. *Environmental Science & Technology* 34, 2513-2517.

Ibáñez, M., Pozo, Ó.J., Sancho, J.V., López, F.J., Hernández, F., 2006. Re-evaluation of glyphosate determination in water by liquid chromatography coupled to electrospray tandem mass spectrometry. *Journal of Chromatography A* 1134, 51-55.

Kazarian, S.G., Chan, K.L.A., 2006. Applications of ATR-FTIR spectroscopic imaging to biomedical samples. *Biochimica et Biophysica Acta (BBA)-Biomembranes* 1758, 858-867.

Kim, M., Son, J., Park, M.S., Ji, Y., Chae, S., Jun, C., Bae, J.-S., Kwon, T.K., Choo, Y.-S., Yoon, H., Yoon, D., Ryoo, J., Kim, S.-H., Park, M.-J., Lee, H.-S., 2013. In vivo evaluation and comparison of developmental toxicity and teratogenicity of perfluoroalkyl compounds using *Xenopus* embryos. *Chemosphere* 93, 1153-1160.

Kupferberg, S.J., 1997. The Role of Larval Diet in Anuran Metamorphosis. *American Zoologist* 37, 146-159.

Kus, S., Marczenko, Z., Obarski, N., Derivative UV-VIS spectrophotometry in analytical chemistry. Llabjani, V., Malik, R.N., Trevisan, J., Hoti, V., Ukpebor, J., Shinwari, Z.K., Moeckel, C., Jones, K.C., Shore, R.F., Martin, F.L., 2012. Alterations in the infrared spectral signature of avian feathers reflect potential chemical exposure: A pilot study comparing two sites in Pakistan. *Environment International* 48, 39-46.

Loumbourdis, N.S., Kyriakopoulou-Sklavounou, P., 1991. Reproductive and lipid cycles in the male frog *Rana ridibunda* in northern Greece. *Comparative Biochemistry and Physiology Part A: Physiology* 99, 577-583.

Lowe-Jinde, L., Niimi, A.J., 1984. Short-term and long-term effects of cadmium on glycogen reserves and liver size in rainbow trout (*Salmo gairdneri* Richardson). *Archives of Environmental Contamination and Toxicology* 13, 759-764.

Maher, J.R., Matthews, T.E., Reid, A.K., Katz, D.F., Wax, A., 2014. Sensitivity of coded aperture Raman spectroscopy to analytes beneath turbid biological tissue and tissue-simulating phantoms. *Journal of biomedical optics* 19, 117001-117001.

Malins, D.C., Anderson, K.M., Stegeman, J.J., Jaruga, P., Green, V.M., Gilman, N.K., Dizdaroglu, M., 2006. Biomarkers signal contaminant effects on the organs of English sole (*Parophrys vetulus*) from Puget Sound. *Environmental Health Perspectives* 114, 823-829.

Malins, D.C., Stegeman, J.J., Anderson, J.W., Johnson, P.M., Gold, J., Anderson, K.M., 2004. Structural changes in gill DNA reveal the effects of contaminants on puget sound fish. *Environmental Health Perspectives* 112, 511-515.

Mann, R., Hyne, R., Choung, C., Wilson, S., 2009. Amphibians and agricultural chemicals: Review of the risks in a complex environment. *Environmental Pollution* 157, 2903-2927.

Mariey, L., Signolle, J.P., Amiel, C., Traver, J., 2001. Discrimination, classification, identification of microorganisms using FTIR spectroscopy and chemometrics. *Vibrational Spectroscopy* 26, 151-159.

Mark, H., Workman Jr, J., 2010. *Chemometrics in spectroscopy*. Academic Press.

Martin, F.L., Kelly, J.G., Llabjani, V., Martin-Hirsch, P.L., Patel, I.I., Trevisan, J., Fullwood, N.J., Walsh, M.J., 2010. Distinguishing cell types or populations based on the computational analysis of their infrared spectra. *Nature Protocols* 5, 1748-1760.

Martínez, A.M., Kak, A.C., 2001. Pca versus Ida. Pattern Analysis and Machine Intelligence, IEEE Transactions on 23, 228-233.

Melvin, S.D., Lanctôt, C.M., Craig, P.M., Moon, T.W., Peru, K.M., Headley, J.V., Trudeau, V.L., 2013. Effects of naphthenic acid exposure on development and liver metabolic processes in anuran tadpoles. Environmental Pollution 177, 22-27.

Mompelat, S., Le Bot, B., Thomas, O., 2009. Occurrence and fate of pharmaceutical products and by-products, from resource to drinking water. Environment International 35, 803-814.

Movasaghi, Z., Rehman, S., ur Rehman, D.I., 2008. Fourier transform infrared (FTIR) spectroscopy of biological tissues. Applied Spectroscopy Reviews 43, 134-179.

Naumann, D., Helm, D., Labischinski, H., 1991. Microbiological characterizations by FT-IR spectroscopy. Nature 351, 81-82.

Neal, C., Jarvie, H.P., Howarth, S.M., Whitehead, P.G., Williams, R.J., Neal, M., Harrow, M., Wickham, H., 2000. The water quality of the River Kennet: Initial observations on a lowland chalk stream impacted by sewage inputs and phosphorus remediation. Science of the Total Environment 251-252, 477-495.

Obinaju, B.E., Alaoma, A., Martin, F.L., 2014. Novel sensor technologies towards environmental health monitoring in urban environments: A case study in the Niger Delta (Nigeria). Environmental Pollution 192, 222-231.

Olivares, A., Quirós, L., Pelayo, S., Navarro, A., Bosch, C., Grimalt, J.O., del Carme Fabregat, M., Faria, M., Benejam, L., Benito, J., 2010. Integrated biological and chemical analysis of organochlorine compound pollution and of its biological effects in a riverine system downstream the discharge point. Science of the Total Environment 408, 5592-5599.

Orton, F., Routledge, E., 2011. Agricultural intensity in ovo affects growth, metamorphic development and sexual differentiation in the Common toad (*Bufo bufo*). Ecotoxicology 20, 901-911.

Orton, F., Tyler, C.R., 2014. Do hormone-modulating chemicals impact on reproduction and development of wild amphibians? Biological Reviews.

Oruç, E.Ö., Üner, N., 1999. Effects of 2,4-Diamin on some parameters of protein and carbohydrate metabolisms in the serum, muscle and liver of *Cyprinus carpio*. Environmental Pollution 105, 267-272.

Palaniappan, P.L.R.M., Vijayasundaram, V., 2008. Fourier transform infrared study of protein secondary structural changes in the muscle of *Labeo rohita* due to arsenic intoxication. Food and Chemical Toxicology 46, 3534-3539.

Palaniappan, P.L.R.M., Vijayasundaram, V., 2009. Arsenic-Induced Biochemical Changes in *Labeo rohita* Kidney: An FTIR Study. Spectroscopy Letters 42, 213-218.

Palaniappan, P.R.M., Vijayasundaram, V., Prabu, S.M., 2011. A study of the subchronic effects of arsenic exposure on the liver tissues of *Labeo rohita* using Fourier transform infrared technique. Environmental Toxicology 26, 338-344.

Pillard, D.A., Cornell, J.S., DuFresne, D.L., Hernandez, M.T., 2001. Toxicity of Benzotriazole and Benzotriazole Derivatives to Three Aquatic Species. Water Research 35, 557-560.

Purna Sai, K., Babu, M., 2001. Studies on *Rana tigerina* skin collagen. Comparative Biochemistry and Physiology Part B: Biochemistry and Molecular Biology 128, 81-90.

Ralph, S., Petras, M., 1997. Genotoxicity monitoring of small bodies of water using two species of tadpoles and the alkaline single cell gel (comet) assay. Environmental and Molecular Mutagenesis 29, 418-430.

Regnery, J., Püttmann, W., 2010. Occurrence and fate of organophosphorus flame retardants and plasticizers in urban and remote surface waters in Germany. Water Research 44, 4097-4104.

Relyea, R.A., Mills, N., 2001. Predator-induced stress makes the pesticide carbaryl more deadly to gray treefrog tadpoles (*Hyla versicolor*). Proceedings of the National Academy of Sciences 98, 2491-2496.

Rieppo, L., Saarakkala, S., Närhi, T., Helminen, H.J., Jurvelin, J.S., Rieppo, J., 2012. Application of second derivative spectroscopy for increasing molecular specificity of Fourier transform infrared spectroscopic imaging of articular cartilage. *Osteoarthritis and Cartilage* 20, 451-459.

Rinnan, Å., Berg, F.v.d., Engelsen, S.B., 2009. Review of the most common pre-processing techniques for near-infrared spectra. *TrAC Trends in Analytical Chemistry* 28, 1201-1222.

Sheridan, M.A., Kao, Y.-H., 1998. Regulation of metamorphosis-associated changes in the lipid metabolism of selected vertebrates. *American Zoologist* 38, 350-368.

Stuart, S.N., Chanson, J.S., Cox, N.A., Young, B.E., Rodrigues, A.S.L., Fischman, D.L., Waller, R.W., 2004. Status and trends of amphibian declines and extinctions worldwide. *Science* 306, 1783-1786.

Taylor, S.E., Cheung, K.T., Patel, I., Trevisan, J., Stringfellow, H.F., Ashton, K.M., Wood, N.J., Keating, P.J., Martin-Hirsch, P.L., Martin, F.L., 2011. Infrared spectroscopy with multivariate analysis to interrogate endometrial tissue: a novel and objective diagnostic approach. *British Journal of Cancer* 104, 790-797.

Tetreault, G.R., McMaster, M.E., Dixon, D.G., Parrott, J.L., 2003. Using reproductive endpoints in small forage fish species to evaluate the effects of Athabasca oil sands activities. *Environmental Toxicology and Chemistry* 22, 2775-2782.

Toyran, N., Lasch, P., Naumann, D., Turan, B., Severcan, F., 2006. Early alterations in myocardia and vessels of the diabetic rat heart: an FTIR microspectroscopic study. *Biochem. J* 397, 427-436.

Trevisan, J., Angelov, P.P., Carmichael, P.L., Scott, A.D., Martin, F.L., 2012. Extracting biological information with computational analysis of Fourier-transform infrared (FTIR) biospectroscopy datasets: current practices to future perspectives. *Analyst* 137, 3202-3215.

Trevisan, J., Angelov, P.P., Scott, A.D., Carmichael, P.L., Martin, F.L., 2013. IRootLab: a free and open-source MATLAB toolbox for vibrational biospectroscopy data analysis. *Bioinformatics*, btt084.

Ukpebor, J., Llabjani, V., Martin, F.L., Halsall, C.J., 2011. Sublethal genotoxicity and cell alterations by organophosphorus pesticides in MCF-7 cells: Implications for environmentally relevant concentrations. *Environmental Toxicology and Chemistry* 30, 632-639.

UKTAG, 2013. Phosphorus standards for rivers—updated recommendations. UK Technical Advisory Group on the Water Framework Directive. .

van der Veen, I., de Boer, J., 2012. Phosphorus flame retardants: Properties, production, environmental occurrence, toxicity and analysis. *Chemosphere* 88, 1119-1153.

Van Stempvoort, D.R., Roy, J.W., Brown, S.J., Bickerton, G., 2014. Residues of the herbicide glyphosate in riparian groundwater in urban catchments. *Chemosphere* 95, 455-463.

Vences, M., Puente, M., Nieto, S., Vieites, D.R., 2002. Phenotypic plasticity of anuran larvae: environmental variables influence body shape and oral morphology in *Rana temporaria* tadpoles. *Journal of Zoology* 257, 155-162.

Venturino, A., Rosenbaum, E., De Castro, A.C., Anguiano, O.L., Gauna, L., De Schroeder, T.F., De D'Angelo, A.M.P., 2003. Biomarkers of effect in toads and frogs. *Biomarkers* 8, 167-186.

Vivó-Truyols, G., Schoenmakers, P.J., 2006. Automatic Selection of Optimal Savitzky-Golay Smoothing. *Analytical Chemistry* 78, 4598-4608.

Williams, P., Whitfield, M., Biggs, J., Bray, S., Fox, G., Nicolet, P., Sear, D., 2004. Comparative biodiversity of rivers, streams, ditches and ponds in an agricultural landscape in Southern England. *Biological Conservation* 115, 329-341.

Xiao, J.P., Zhou, Q.X., Tian, X.K., Bai, H.H., Su, X.F., 2007. Determination of aniline in environmental water samples by alternating-current oscillopolarographic titration. *Chinese Chemical Letters* 18, 730-733.

Zaya, R.M., Amini, Z., Whitaker, A.S., Kohler, S.L., Ide, C.F., 2011. Atrazine exposure affects growth, body condition and liver health in *Xenopus laevis* tadpoles. *Aquatic Toxicology* 104, 243-253.

Álvarez, D., Nicieza, A.G., 2002. Effects of temperature and food quality on anuran larval growth and metamorphosis. *Functional Ecology* 16, 640-648.

**Figure 1**

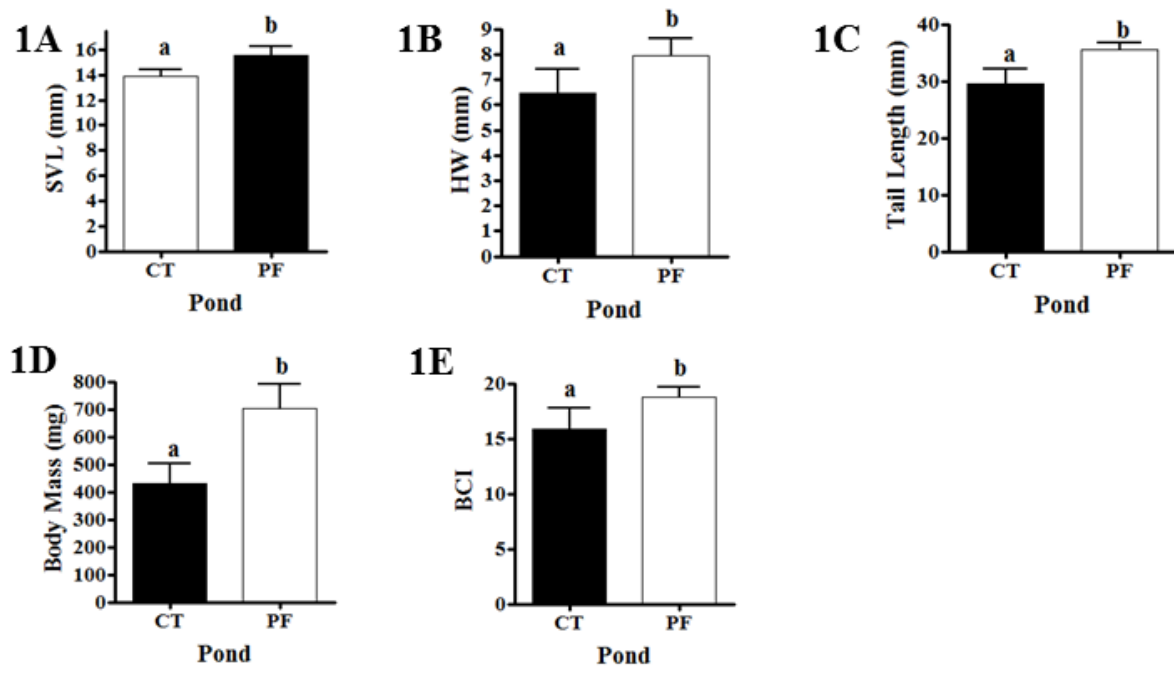
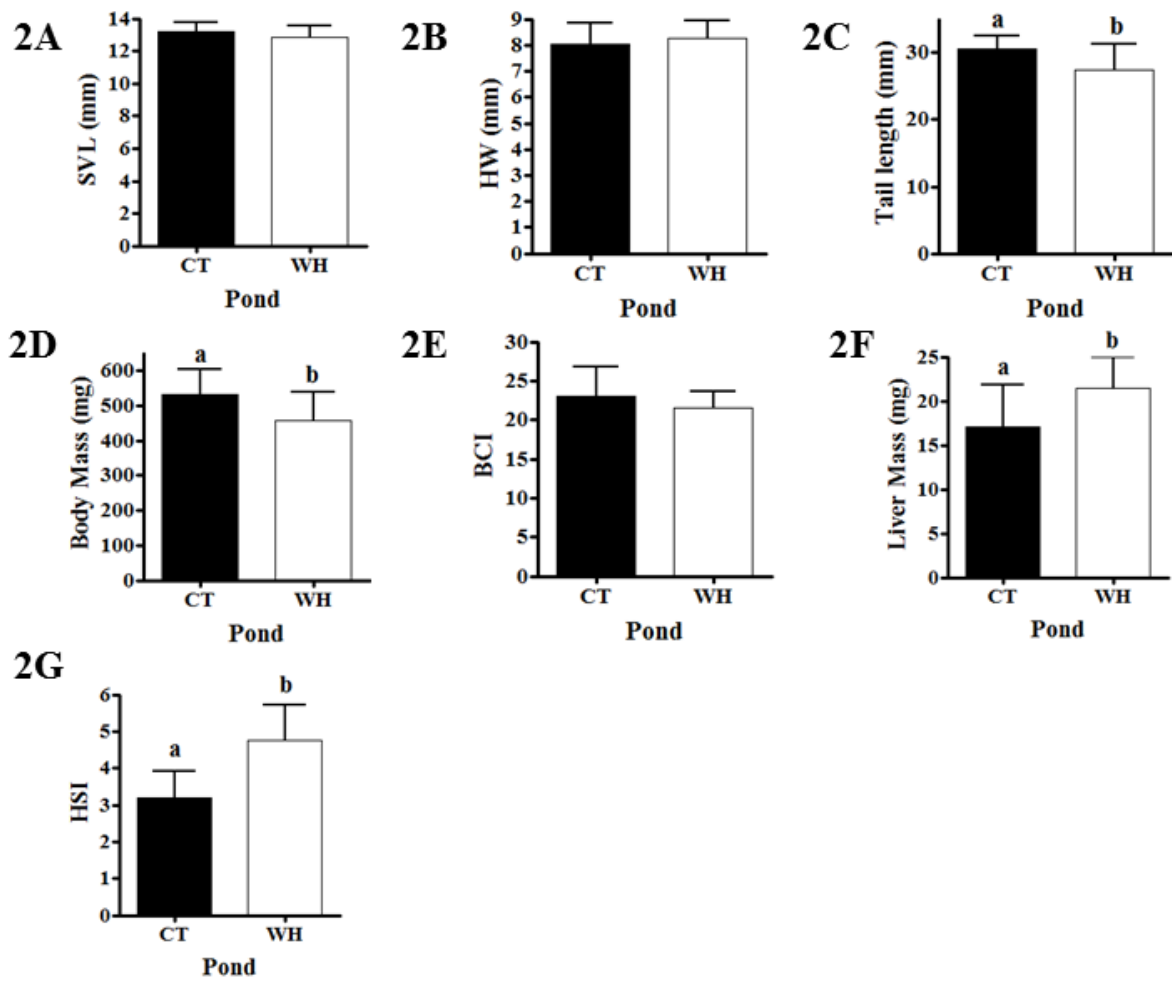
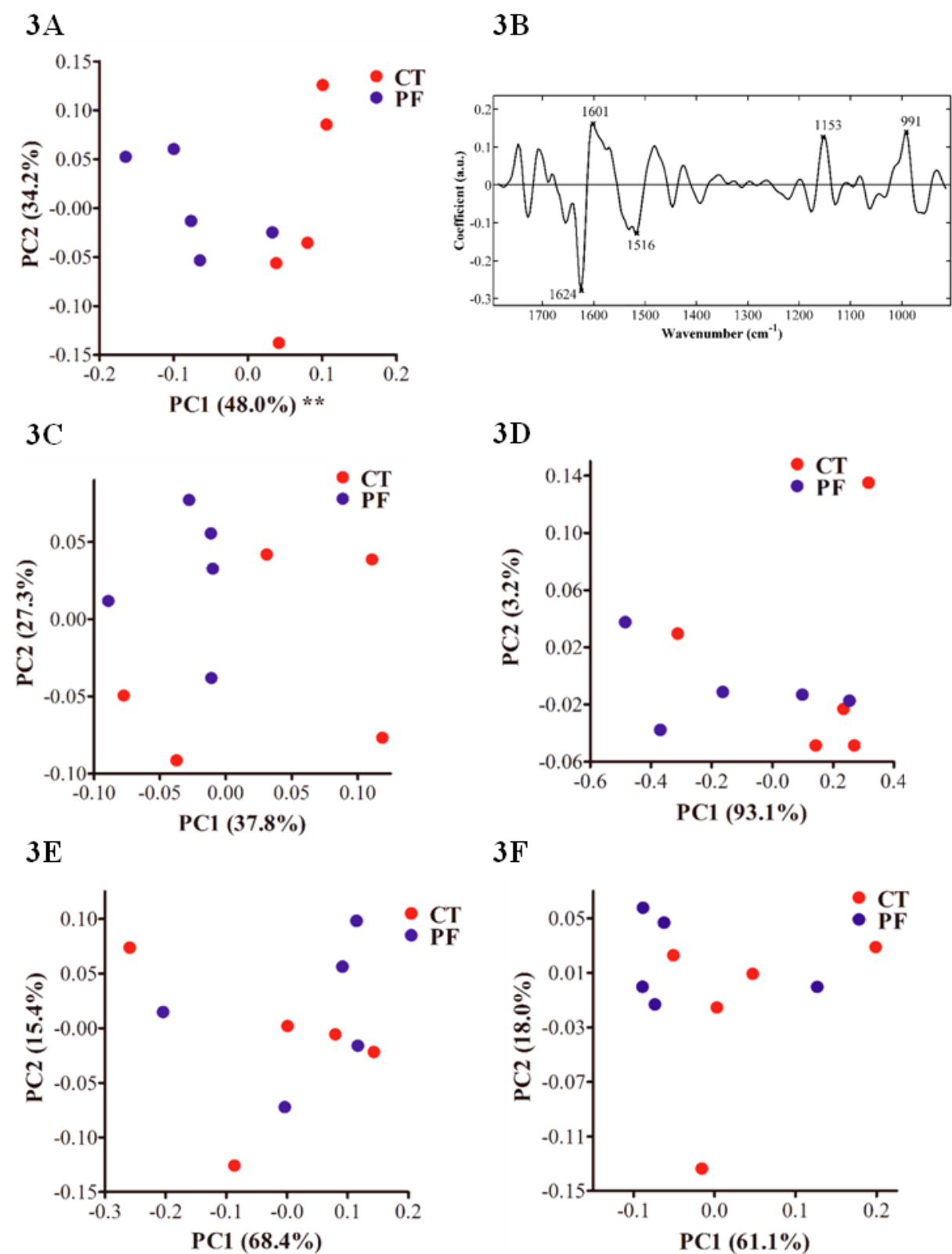


Figure 2



**Figure 3**



**Figure 4**

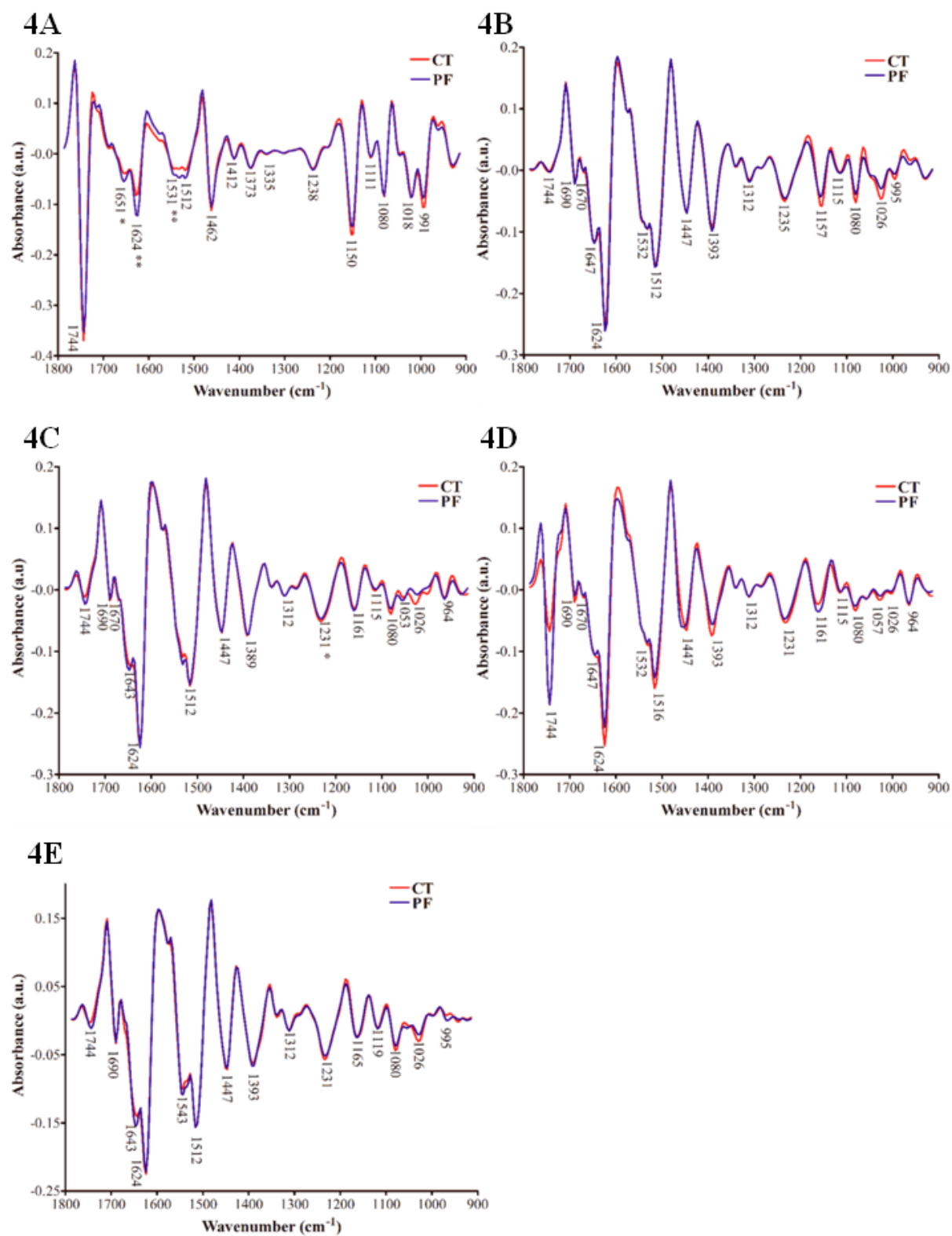




**Figure 5**

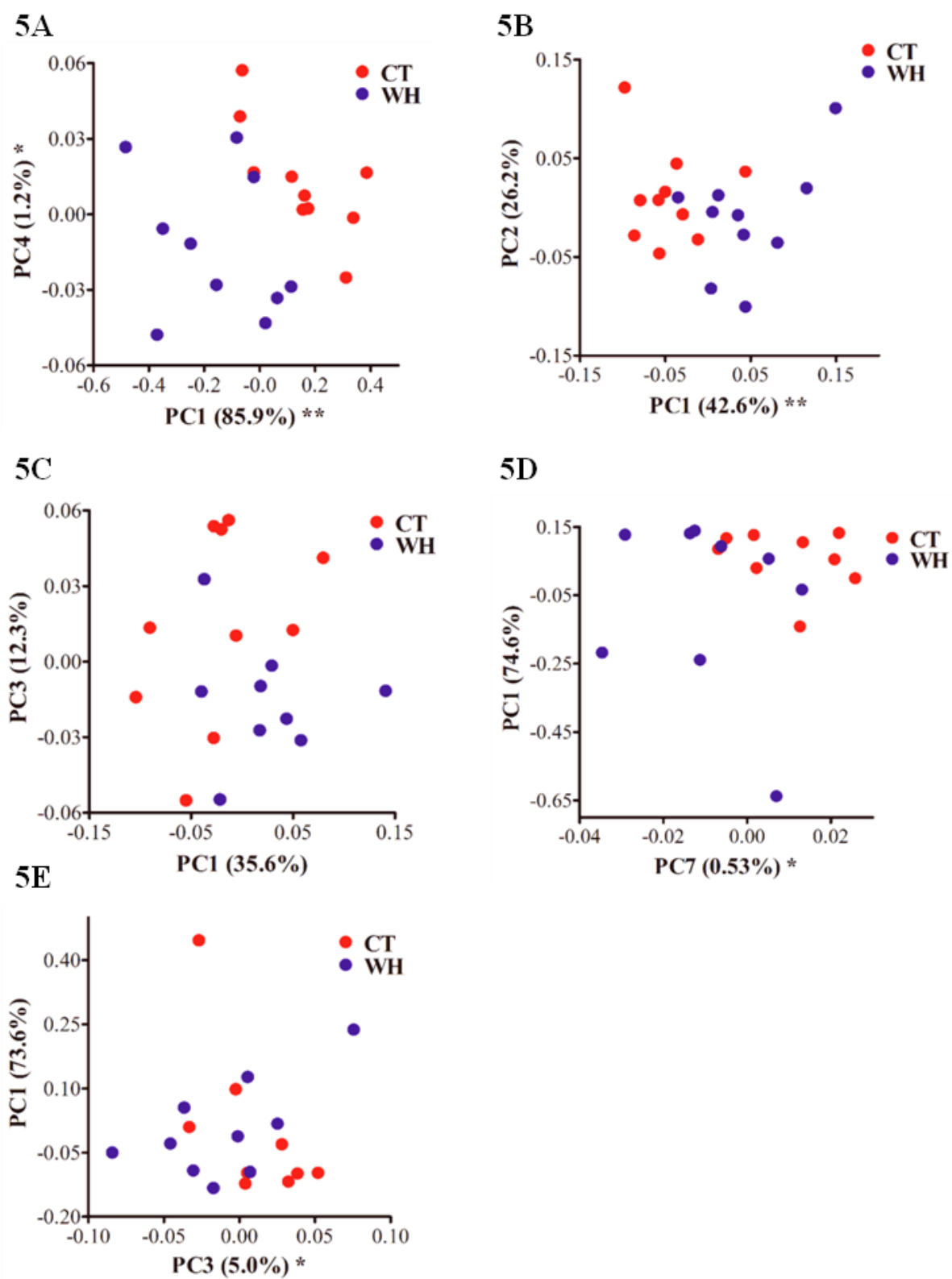
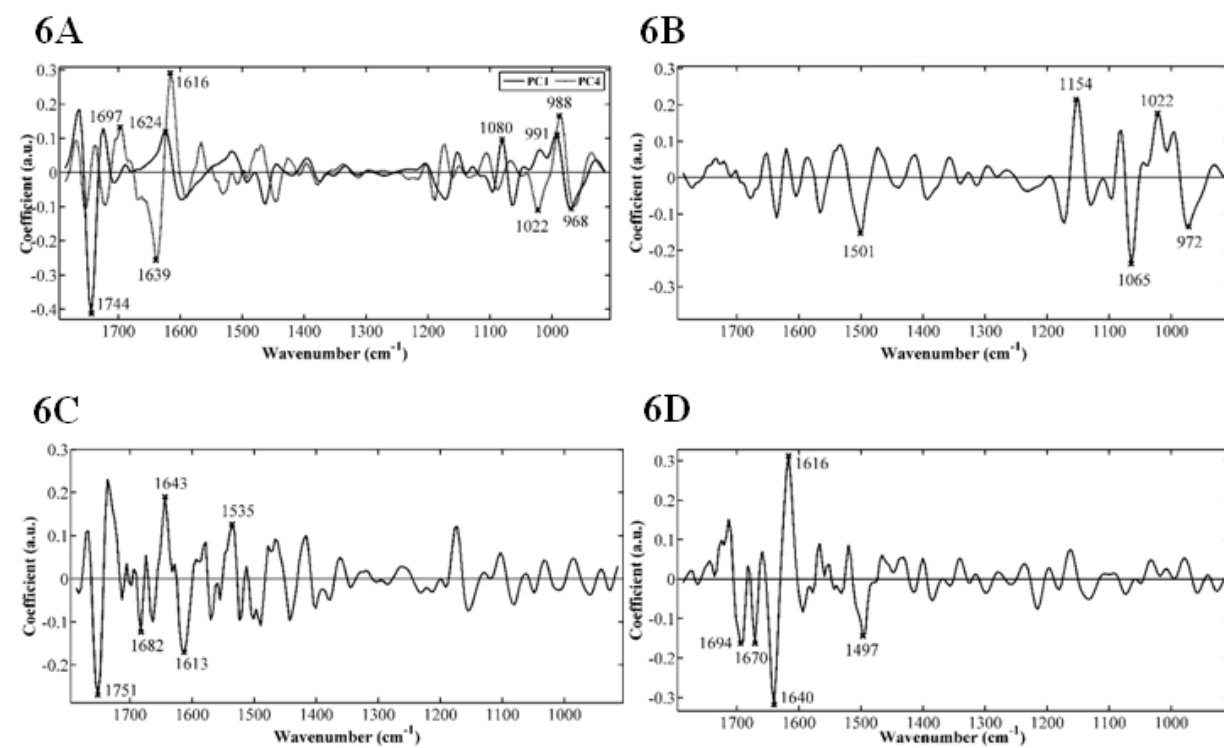


Figure 6



**Figure 7**

